Published in final edited form as:

Mol Immunol. 2022 August ; 148: 6–17. doi:10.1016/j.molimm.2022.05.009.

Regulation and function of Id2 in plasmacytoid dendritic cells

Rachel L. Babcock[a,b], **Yifan Zhou**[a], **Bhakti Patel**[a], **Taylor T. Chrisikos**[a,b], **Laura M. Kahn**[a,b], **Allison M. Dyevoich**[a], **Yusra B. Medik**[a], **Stephanie S. Watowich**[a,b]

[a]Department of Immunology, The University of Texas MD Anderson Cancer Center, Houston, TX, 77030, USA

[b]The University of Texas MD Anderson Cancer Center UT Health Graduate School of Biomedical Sciences, Houston, TX, 77030, USA

Abstract

Plasmacytoid dendritic cells (pDCs) are specialized type I interferon (IFN-I) producing cells that promote anti-viral immune responses and contribute to autoimmunity. Development of pDCs requires the transcriptional regulator E2-2 and is opposed by inhibitor of DNA binding 2 (Id2). Prior work indicates *Id2* is induced in pDCs upon maturation and may affect pDC IFN-I production via suppression of E2-2, suggesting an important yet uncharacterized role in this lineage. We found TLR7 agonists stimulate Id2 mRNA and protein expression in pDCs. We further show that transcriptional activation of *Id2* is dependent on the E2 ubiquitin-conjugating enzyme Ubc13, but independent of IFN-I signaling in response to TLR7 agonist stimulation. Nonetheless, conditional *Id2* depletion in pDCs indicates Id2 is dispensable for TLR7 agonist-induced maturation and inhibition of E2-2 expression. Thus, we identify new mechanisms of Id2 regulation by Ubc13, which may be relevant for understanding Id2 gene regulation in other contexts, while ruling out major roles for Id2 in pDC responses to TLR7 agonists.

Keywords

pDCs; TLR; Id2; Ubc13; IFNAR signaling; soluble factors

1. Introduction

Dendritic cells (DCs) are bone marrow (BM)-derived populations comprising plasmacytoid DCs (pDCs), as well as the type 1 and type 2 conventional DCs (cDC1s and cDC2s) (Chrisikos et al., 2019; Guilliams et al., 2014; Steinman and Cohn, 1973). Murine and human DCs express a variety of receptors that detect pathogen-, danger-, or microbial-associated molecular patterns including the Toll-like receptors (TLRs) (Chrisikos et al.,

Corresponding author: Stephanie S. Watowich, Ph.D., Department of Immunology, The University of Texas MD Anderson Cancer Center, P.O. Box 301402, Unit 902, Houston, TX 77030, USA. Fax: +01 713-563-3357; swatowic@mdanderson.org.

Author contributions

Conception and design of the study, R.L.B. and S.S.W.; Formal analysis, R.L.B.; Funding acquisition, S.S.W.; Investigation, R.L.B., Y.Z., B.P., T.T.C., L.M.K., A.M.D., and Y.B.M.; Supervision, S.S.W.; Visualization, R.L.B. and S.S.W.; Writing – original draft, R.L.B. and S.S.W.; Writing – review and editing, R.L.B., Y.Z., B.P., T.T.C., L.M.K., A.M.D., Y.B.M., and S.S.W.

Declaration of Competing Interests

The authors declare that they have no competing interests.

2019). TLR activation leads to changes in DC phenotype, including upregulation of major histocompatibility complex class II (MHC-II), co-stimulatory molecules, and soluble factors, a process that is termed DC maturation (Chrisikos et al., 2019). pDCs are enriched for expression of the nucleic acid sensors TLR7 and TLR9; upon their activation, pDCs produce abundant amounts of type I interferons (IFN-Is) and contribute to antiviral immunity. pDCs also produce other pro-inflammatory cytokines, but exhibit limited antigen presentation capacity (Cella et al., 1999; Reizis, 2019; Siegal et al., 1999; Swiecki and Colonna, 2015). By contrast, cDCs are phagocytic cells that acquire potent antigen-presenting function following TLR activation (Böttcher and Reis e Sousa, 2018; Hilligan and Ronchese, 2020). TLR agonist-stimulated pDCs and cDC1s have been studied in recent years for potential use as cell-based vaccines in the treatment of various cancers (Chrisikos et al., 2020; Liu et al., 2008; Wu et al., 2017; Zhou et al., 2020). Thus, it is important to elucidate mechanisms by which DCs respond to TLR ligands to better understand fundamental DC biology and improve DC-based immunotherapies.

DC development is controlled by key transcriptional regulators, including the E protein E2-2 and inhibitor of DNA binding 2 (Id2) (Cisse et al., 2008; Grajkowska et al., 2017; Hacker et al., 2003; Nagasawa et al., 2008; Spits et al., 2000). E2-2 and Id2 are helix-loop-helix (HLH) proteins, which form homo or heterodimers via the HLH region (Murre, 2019; Murre et al., 1989a, 1989b). E proteins such as E2-2 (encoded by *Tcf4*) also contain a basic region that enables their direct binding to DNA at consensus E-box sites to regulate gene expression (Church et al., 1985; Ephrussi et al., 1985; Robert.L et al., 1990). By contrast, Id proteins including Id2 lack a basic region (Benezra et al., 1990). Id proteins dimerize with and inhibit E protein DNA binding and thus act as dominant negative regulators of transcription (Benezra et al., 1990; Kee, 2009). In DCs, antagonism between E2-2 and Id2 directs pDC and cDC1 development (Cisse et al., 2008; Grajkowska et al., 2017; Hacker et al., 2003; Nagasawa et al., 2008; Spits et al., 2000). For instance, the long isoform of E2-2 acts in conjunction with its co-factor Cbfa2t3 in a feed-forward loop to sustain E2-2- and pDC-specific gene expression while concomitantly repressing *Id2*; this mechanism promotes pDC development from DC progenitors and maintains pDC lineage identity (Ghosh et al., 2014; Grajkowska et al., 2017). In addition, evidence suggests Id2 silences E protein-dependent pDC potential within the DC progenitor compartment while promoting pre-cDC1 and cDC1 development (Bagadia et al., 2019; Grajkowska et al., 2017; Nagasawa et al., 2008; Spits et al., 2000).

pDCs express E2-2 constitutively and sustained E2-2 expression is required for maintenance of pDC phenotype and morphology (Ghosh et al., 2010). We previously showed pDCs stimulated with the TLR9 agonist CpG-A upregulate *Id2* mRNA (Li et al., 2012), suggesting Id2 may control specific pDC functions. TLR agonists, viral infection, or CD40 ligand (CD40L) stimulation drive pDC maturation, including production of IFN-Is and pro-inflammatory factors. This process results in subsequent acquisition of cDC-like features by pDCs, including upregulation of MHC-II and co-stimulatory molecules, and ability to induce T cell activation (Asselin-Paturel et al., 2001; Iparraguirre et al., 2007; Mouriès et al., 2008; O'Keeffe et al., 2002; Salio et al., 2004; Schlecht et al., 2004). Additionally, pDCs exposed to virus or CD40L induce *Id2* (Abbas et al., 2020; Iparraguirre et al., 2007; Leylek et al., 2020). Furthermore, *Tcf4* (E2-2) -deficient pDCs exhibit features similar to

TLR agonist-treated pDCs, including loss of pDC-specific gene expression, enrichment of cDC-associated transcripts including *Id2*, reduced IFN-α production, and enhanced ability to stimulate T cells (Cisse et al., 2008; Ghosh et al., 2010). Prior work has also shown *Id2*-deficient pDCs produce greater amounts of IFN-α following exposure to virus (Hacker et al., 2003). These results collectively suggest TLR agonist-induced Id2 may antagonize the E2-2-dependent transcriptional program in pDCs and support maturation to a cDC-like state; yet, the role of Id2 in TLR agonist-stimulated pDCs remains unknown.

All TLRs, except for TLR3, signal through MyD88 and TRAF6, which in turn elicit NF-κB and MAP kinase signal transduction cascades (Kawasaki and Kawai, 2014). The E2 ubiquitin-conjugating enzyme Ubc13 (encoded by *Ube2n*) has a crucial role in TRAF6 activation and thus is important for signaling via the majority of TLRs (Deng et al., 2000; Fitzgerald and Kagan, 2020; Fukushima et al., 2007; Hofmann and Pickart, 1999). Moreover, TLR7 and TLR9 signaling activates IRF7-dependent IFN-I production and autocrine/paracrine IFN-α/β receptor (IFNAR) signaling (Asselin-Paturel et al., 2005; Honda et al., 2005; Tomasello et al., 2018; Wimmers et al., 2018). Since *Id2* is upregulated in pDCs by TLR9 agonist or viral challenge, the data collectively suggest *Id2* is transcriptionally regulated by TLR-mediated signaling pathways, yet the mechanisms by which *Id2* is controlled in response to TLR stimulation remains unclear.

In this study, we used gene expression and protein analyses to verify Id2 induction by TLR agonist treatment in murine pDCs. We further examined roles for Id2 in pDC maturation and cytokine expression using conditional *Id2* deletion. Finally, we employed *in vitro* analyses and genetic models to assess mechanisms regulating *Id2* gene expression following TLR7 stimulation.

2. Materials and Methods

2.1. Animals

C57BL/6J mice and B6.129S2-*Ifnar1*^{tm1Agt}/Mmjax (*Ifnar*$^{-/-}$) mice (Müller et al., 1994) were bred in house or acquired from the Jackson Laboratory (Bar Harbor, ME, USA). Non-littermate C57BL/6J mice were used as wildtype controls. *Id2* conditional knockout mice (*Id2*^{CKO}; CreERT2$^{+/+}$ *Id2*$^{f/f}$ or CreERT2$^{+/-}$ *Id2*$^{f/f}$) were generated by breeding B6.129-*Gt(ROSA)26Sor*$^{tm1(cre/ERT2)Tyj}$/J mice (CreERT2$^{+/+}$) from the Jackson Laboratory (Ventura et al., 2007) with *Id2*$^{f/f}$ mice (Niola et al., 2012); the latter were generously provided on the C57BL/6J background by Drs. Anna Lasorella and Barbara Kee. Conditional *Ube2n* knockout mice (*Ube2n*^{CKO}; CreERT2$^{+/+}$ *Ube2n*$^{f/f}$) were obtained by breeding CreERT2$^{+/+}$ mice with *Ube2n*$^{f/f}$ mice on the C57BL/6J background (Yamamoto et al., 2006). Non-littermate CreERT2$^{+/+}$ mice were used as controls for both the *Id2*^{CKO} and *Ube2n*^{CKO} strains. Mice were age-matched and used between 7-16 weeks of age. Mice were maintained in a specific pathogen-free barrier facility and used in accordance with approval by The University of Texas MD Anderson Cancer Center's Institutional Animal Care and Use Committee (IACUC).

2.2. Immune cell isolation

Mice were euthanized via CO_2 asphyxiation; secondary cervical dislocation was performed to ensure animals were ethically euthanized. Peripheral blood was collected via cardiac puncture. BM was harvested from both hind legs (2 femurs and 2 tibias and, in some cases, 2 humeri), and flushed using a 27.5-gauge needle. BM was incubated with RBC lysis buffer (Tonbo Biosciences, San Diego, CA, USA) for 5 min at room temperature (RT); the reaction was stopped with the addition of Roswell Park Memorial Institute (RPMI) complete medium, consisting of RPMI 1640 medium (Thermo Fisher Scientific, Waltham, MA, USA) containing 10% heat-inactivated fetal calf serum (FCS, Atlanta Biologicals, Atlanta, GA, USA), 1% penicillin-streptomycin (Thermo Fisher Scientific), 1 mM sodium pyruvate (Thermo Fisher Scientific), and 50 μM β-mercaptoethanol (β-ME, Thermo Fisher Scientific). Total BM cells were passed through a 70 μm mesh filter and pelleted by centrifugation. Cells were resuspended in either fluorescence-activated cell sorting (FACS) buffer, comprising phosphate-buffered saline (PBS) containing 2 mM ethylenediaminetetraacetic acid and 2% FCS (FACS buffer) for antibody staining, or RPMI complete medium for BM cultures. Spleen was pressed through 100 μm mesh filters, and single cell suspensions were incubated with RBC lysis buffer, as described. Lymph nodes were pressed through 100 μm mesh filters into single cell suspensions. The large lobe of the liver was chopped by hand with scissors into uniformly small pieces, then incubated for 1-1.5 h at 37°C while shaking with 1 mg/mL collagenase-IV in RPMI complete medium containing 1X Hanks balanced salt solution (Sigma Aldrich). Liver digests were passed through a 40 μm mesh filter and immune cells were enriched using a 37/70% Percoll® gradient (Cytiva, Marlborough, MA, USA); cells at the 37/70 interface were collected and washed with PBS. All single cell suspensions were resuspended in FACS buffer prior to antibody staining.

2.3. Fluorescence-activated cell sorting (FACS) and flow cytometry

Single cell suspensions were collected, washed with FACS buffer, then incubated with FACS buffer containing rat anti-mouse CD16/23 antibody (Fc-block, Tonbo Biosciences) for 10-15 min on ice. Cells were subsequently stained with fluorescently-conjugated antibodies against cell surface molecules for 20-30 min on ice in combination with Ghost Dye™ violet (Tonbo Biosciences); the latter was used to exclude dead cells. The following antibodies were used: FITC-conjugated CD11b (M1/70), CD11c (N418), CD80 (16-10A1), CD172α (P84), H-2Kb (AF6-88.5), and Siglec-H (eBio440c); PerCP-conjugated CD86 (GL-1); PerCP-Cy5.5-conjugated CD3 (17A2), CD11b (M1/70), CD19 (1D3), CD24 (M1/69), CD80 (16-10A1), F4/80 (BM8), NKp46 (29A1.4), NK1.1 (PK136), and XCR1 (ZET); Brilliant Violet (BV)421™-conjugated XCR1 (ZET); eFluor 450-conjugated CD11c (N418); violetFluor™ 450-conjugated CD11b (M1.70), CD11c (N418); Pacific Blue™-conjugated CD40 (3/23); BV650™-conjugated CD11c (HL3); BV711™-conjugated CD8α (17A2), CD45R (RA3-6B2), and CD274 (MIH5); BV785™-conjugated CD86 (GL-1); PE-conjugated CCR7 (4B12), CCR9 (eBioCW-1.2), CD11b (M1/70), CD103 (2E7), and Siglec-H (eBio440c); PE-Cy7-conjugated CD11c (N418), CD45R (RA3-6B2), CD86 (GL-1), Siglec-H (eBio440c), MHC-II (M5/114.15.2); APC-conjugated CD45R (RA3-6B2), CD172α (P84), and CD317 (eBio927); Red Fluor710-conjugated CD45.2 (104); APC-Cy7-conjugated CD11b (M1/70) and MHC-II (M5/114.15.2); APC-eFluor 780-conjugated CD24

(M1/69). Antibodies were purchased from Thermo Fisher Scientific (Invitrogen), Tonbo Biosciences, BioLegend (San Diego, CA, USA), or BD. Following staining, cells were washed with FACS buffer, and either filtered through a 40 μm mesh filter and sorted at 4°C using a FACSAria IIIu or FACSAria Fusion Cell Sorter (Beckton, Dickinson and Company (BD), Franklin Lakes, NJ, USA), and the BD FACSDiva™ software (BD), or fixed in PBS containing 2.5% formaldehyde for 20 min on ice. Fixed cells were washed and resuspended in FACS buffer prior to data acquisition using a BD LSR Fortessa X-20 Analyzer (BD) and BD FACSDiva™ software. Data were analyzed using the FlowJo v10 software (FlowJo, Ashland, OR, USA).

2.4. DC cultures *in vitro*

Murine BM-derived pDCs and CD103$^+$ cDC1s were generated *in vitro* as described (Chrisikos et al., 2020; Li et al., 2012; Zhou et al., 2020). To differentiate pDCs, BM cells (3x10^6 cells/mL) were cultured in RPMI complete medium supplemented with 50 ng/mL human FMS-like tyrosine kinase 3 (Flt3) ligand (hFlt3L; PreproTech, Rocky Hill, NJ, USA) for 8 d. At culture termination, non-adherent cells were gently collected; pDCs were purified as live CD11c$^+$ CD11b$^-$ B220$^{+/hi}$ Siglec-H$^+$ or PDCA1$^+$ CD24$^{-/lo}$ MHC-II$^{-/lo}$ cells by FACS. Cultures generated from tamoxifen-inducible CreER mouse strains were supplemented with 1μM 4-hydroxytamoxifen (4-OHT; Millipore Sigma, St. Louis, MO, USA) on day 4.

To generate CD103$^+$ cDC1s, BM cells (1.5x10^6 cells/mL) were cultured in 10 mL RPMI complete medium containing 50 ng/mL Flt3L and 0.5% XG3 cell supernatant containing granulocyte-macrophage colony-stimulating factor (GM-CSF), or 50 ng/mL Flt3L and 2 ng/mL recombinant murine GM-CSF (PreproTech) for 16-17 d. On day 5, cultures were supplemented with fresh RPMI complete medium. On day 9, non-adherent cells were collected and re-plated in fresh cytokine-supplemented RPMI complete medium (3x10^5 cells/mL). On days 16-17, non-adherent cells were collected; CD103$^+$ cDC1s were purified as live CD11c$^+$ B220$^-$ CD172α$^-$ CD24$^+$ CD103$^+$ cells by FACS.

2.5. Plasmid isolation, hydrodynamic gene transfer (HGT), and DC expansion *in vivo*

The pORF expression vectors encoding the murine *Flt3l* open reading frame (pORF9-mFlt3L; InvivoGen, San Diego, CA, USA) or *Csf2* (GM-CSF) (pORF9-mGM-CSF) were transformed into *E. coli* and grown in lysogeny broth (LB) media with 100 μg/mL ampicillin for 14-16 h. Plasmids were purified using the Invitrogen PureLink HiPure Plasmid Midiprep or Maxiprep Kit (REF: K210004 or F210007; Thermo Fisher Scientific).

Mice were injected intravenously (i.v.) for 5 s via hydrodynamic gene transfer (HGT) (Liu et al., 1999) with 10 μg pORF9-mFlt3L resuspended in 2 mL endotoxin-free Dulbecco's PBS without calcium or magnesium (EMD Millipore) (Li et al., 2012). 7-10 d after Flt3L-HGT, mice were sacrificed and organs were collected and processed as described in the text or figure legends. BM and splenic pDCs were purified as lineage (Lin)$^-$ (CD3, CD19, F4/80) CD11c$^{lo/int}$ CD11b$^-$ Siglec-H$^+$ B220$^{+/hi}$ cells and, in the majority of cases, additionally as NK1.1$^-$ or NKp46$^-$ XCR1$^-$ CD172α^{lo} cells to further exclude possible contaminating NK cells or cDCs. To generate non-lymphoid organ CD103$^+$ cDC1s, mice were injected i.v.

via HGT with 10 μg pORF9-mFlt3L and 2.5 μg pORF9-mGM-CSF resuspended in 2 mL endotoxin-free PBS. Livers were harvested 7-10 d post-HGT. Liver $CD103^+$ cDC1s were sorted as $CD45^+$ Lin- (CD3, CD19, F4/80) $CD11c^+$ $MHC\text{-}II^+$ $CD172\alpha^-$ $XCR1^+$ $CD103^+$ cells.

2.6. TLR agonist, Actinomycin D, or cytokine treatment *in vitro*

FACS-purified cells were washed with RPMI, and then cultured in RPMI complete medium with or without TLR agonists and, in some cases, cytokines. pDCs (0.035-3 x 10^6 cells/mL) were stimulated with R837 (5 μg/mL; InvivoGen), CpG-A (1 μM; sequence: G*G*TGCATCGATGCAG*G*G*G*G*G), heat-inactivated (56°C for 30 minutes) influenza A/PR/8/34 virus (multiplicity of infection (MOI) 50; ATCC, Manassas, VA, USA), Actinomycin D (AcD, 5 μg/mL; Thermo Fisher Scientific), or recombinant mouse IFN-α (300 units; R&D Systems, Inc., Minneapolis, MN, USA). $CD103^+$ cDC1s (2x10^6 cells/mL) were stimulated with lipopolysaccharide (LPS, 100 ng/mL; ultrapure LPS from *E. coli* O111:B4; InvivoGen) or polyinosinic:polycytidylic acid (poly I:C, 20 μg/mL; Millipore Sigma, Darmstadt, Germany). When pDCs were stimulated for greater than 8 h, cultures were supplemented with 50 ng/mL hFlt3L to preserve cell viability; similarly, $CD103^+$ cDC1s cultured greater than 8 h were supplemented with 50 ng/mL hFlt3L and 2 ng/mL GM-CSF.

2.7. RNA isolation and qRT-PCR

Total RNA was isolated from single cell suspensions using TRIzol reagent (Thermo Fisher Scientific) and reverse-transcribed into cDNA with iScript (Bio Rad, Hercules, CA, USA). Quantitative real time polymerase chain reaction (qRT-PCR) was performed using SYBR Green JumpStart Taq ReadyMix (Millipore Sigma) or PowerUp™ SYBR™ Green Master Mix (Thermo Fisher Scientific) and the CFX96 or CXF384 Touch™ Real-Time PCR Detection System with the CFX manager software (Bio Rad) according to the following protocol: denaturation at 95°C for 10 s; annealing at 58°C for 20 s; and extension at 72°C for 30 s. The primer sequences are found in Table 1. The relative expression of individual genes was calculated and normalized to expression of the ribosomal protein L13a gene, *Rpl13a*, using the equation 1.8^(*Rpl13*a - *Gene*) x 10,000, where *Rpl13a* equaled the average threshold cycle (Ct) value for *Rpl13a* mRNA and *Gene* equaled the average Ct value for the gene of interest.

2.8. Sodium dodecyl-sulfate polyacrylamide gel electrophoresis (SDS-PAGE) and immunoblotting

Cells were pelleted and resuspended in 2X Laemmli sample buffer (LSB; 2% SDS, 80mM Tris pH=6.8, 15% glycerol, ~0.01% bromophenol blue) at a concentration of 5x10^5 cells per 50 μL LSB containing 1% β-ME. Samples were sonicated on ice, using the W-385 Heat Systems Ultrasonic processor, at 40% power, for 2 s pulses over 10 s, and boiled for 5 min at 95°C to generate denatured whole cell lysates. 7.5%, 10%, or 15% 1.5 mm polyacrylamide gels were cast for SDS-PAGE using a HOEFER Vertical tank (DD BioLab, Barcelona, Spain). Proteins were transferred to a 100% pure Whatman® Protran® nitrocellulose membrane (0.2 μM, Sigma) overnight at 4°C. Membranes were incubated with primary antibodies overnight at 4°C, diluted as indicated in blocking buffer containing 5% bovine

serum albumin (BSA) or non-fat milk prepared in Tris-buffered saline containing 0.15% Tween-20 (TBST), to detect: Id2 (1:500, D39E8; Cell Signaling Technology, Danvers, Massachusetts, USA); TCF4 (E2-2) (1:1000, Proteintech Group, Inc, Rosemont, IL, USA); Y701-phosphorylated STAT1 (pSTAT1, 1:000, 58D6; Cell Signaling Technology); total STAT1 (1:1000, Cell Signaling Technology); GAPDH (1:10,000, 14C10; Cell Signaling Technology); and tubulin (1:1000, clone 12G10). Membranes were then washed three times for 5 min each with TBST, and incubated while shaking with appropriate horseradish peroxidase-conjugated secondary antibodies in blocking solution for 1 h at RT. Following washes and incubation with SuperSignal West Pico PLUS Chemiluminescent Substrate (Thermo Fisher Scientific), protein expression was detected via x-ray film exposure.

2.9. Cytokine and chemokine quantification

Cell culture supernatants were collected as indicated in the Figure legends and 36 cytokines and chemokines were measured using the mouse ProcartaPlex Panel 1a (Invitrogen, Carlsbad, CA, USA) on a Luminex 200 machine (Luminex, Austin, TX, USA), according to the manufacturers' instructions. Soluble factors measured included: CC motif chemokine ligand 2 (CCL2), CCL3, CCL4, CCL5, CCL7, C-X-C motif chemokine ligand 1 (CXCL1), CXCL2, CXCL5, CXCL10, Eotaxin, granulocyte colony-stimulating factor (G-CSF), GM-CSF, IFN-α, IFN-γ, interleukin-1 alpha (IL-1α), IL-1β, IL-2, IL-3, IL-4, IL-5, IL-6, IL-9, IL-10, IL-12p70, IL-13, IL-15/IL-15R, IL-17a, IL-18, IL-22, IL-23, IL-27, IL-28, IL-31, leukemia inhibitory factor (LIF), macrophage colony-stimulator factor (M-CSF), and tumor necrosis factor alpha (TNF-α).

2.10. Statistics

All statistical analyses performed in this study used Prism 9 software (GraphPad Software, San Diego, CA, USA). A Students *t*-test was used to calculate the difference between two independent groups. When more than two groups were compared, a one-way or two-way analysis of variance (ANOVA), followed by Dunnett's, Bonferroni's or Tukey's multiple comparisons test was performed. Data were expressed as the mean ± standard error of the mean (SEM) of n biological replicates. Results were considered significant when $p < 0.05$.

3. Results

3.1. Id2 expression is upregulated while E2-2 is reduced in TLR agonist-stimulated pDCs

To examine Id2 expression in pDCs, we used two independent methods to generate this rare population of cells. Our first approach employed murine bone marrow (BM) cultures containing Flt3 ligand (Flt3L) to generate pDCs *in vitro* (S1A). The second approach used hydrodynamic gene transfer (HGT) with Flt3L-encoding plasmid to expand pDCs *in vivo* (Fig 1A,B; Fig S1B) (Li et al., 2012; Liu et al., 1999). We also generated $CD103^+$ cDC1s as *Id2*-expressing controls, using *in vitro* cultures or Flt3L HGT (Fig S1C,D) (Chrisikos et al., 2020; Zhou et al., 2020). As expected, we found constitutive expression of *Id2* was lower in pDCs compared to cDC1s, while *Tcf4* (E2-2) was enriched in pDCs versus cDC1s (Fig S1E,F).

Following stimulation of *in vitro*-differentiated pDCs with the TLR7 agonist R837 or the TLR9 agonist CpG-A, we observed induction of *Id2* mRNA (Fig S2A; data not shown), corroborating and extending our previous findings (Li et al., 2012). We confirmed *Id2* induction in R837-stimulated pDCs following expansion *in vivo*, while *Id2* showed a trend for upregulation in response to CpG-A (Fig 1C,D; Fig S2B,C). TLR7/9 agonist-treated pDCs also upregulated *Ifna*, indicating canonical response to these ligands (Fig S2B,D; data not shown). By contrast, *Id2* was reduced in $CD103^+$ cDC1s upon stimulation with the TLR3 agonist polyinosinic-polycytidylic acid (poly I:C), while it was unaffected by LPS treatment (Fig S2E). To assess whether pDCs also upregulated Id2 protein, we used immunoblotting experiments. These assays showed Id2 accumulated in pDCs by 18 h of TLR7 or TLR9 stimulation (Fig 1E; Fig S2F). Collectively, our data indicate Id2 expression is induced in murine pDCs following stimulation with TLR7 or TLR9 agonists.

Numerous studies have found pDCs treated with TLR agonists, as well as CD40L or virus, downregulate *Tcf4*; in some cases, pDCs also simultaneously upregulate *Id2* (Abbas et al., 2020; Alcántara-Hernández et al., 2017; Cisse et al., 2008; Ghosh et al., 2010; Leylek et al., 2020; Macal et al., 2018). Since Id2 antagonizes E protein activity (Benezra et al., 1990; Kee, 2009), we assessed E2-2 expression in R837-stimulated pDCs. *Tcf4* mRNA, the long isoform of E2-2 ($E2\text{-}2_L$), which is specific to pDCs and required for *Tcf4* autoregulation (Grajkowska et al., 2017), as well as the short isoform ($E2\text{-}2_S$) were reduced in response to R837 (Fig 1F,G; Fig S2D). These data demonstrate concomitant induction of Id2 and suppression of E2-2 in R837-stimulated pDCs.

3.2. Id2 does not regulate *Tcf4* or E2-2 target gene expression in TLR7-stimulated pDCs

Since R837 stimulation resulted in significant upregulation of Id2 (Fig 1), we focused our efforts on understanding whether Id2 affects the response of pDCs to distinct TLR7 agonists including R837 and heat-inactivated influenza virus. We generated pDCs from CreER $Id2^{f/f}$ mice ($Id2^{CKO}$) and CreER (control) BM *in vitro*. Cells were stimulated with TLR7 agonists; some cultures were also treated with 4-OHT to promote Cre activity and *Id2* gene deletion. We verified Id2 mRNA and protein depletion in the $Id2^{CKO}$ cultures treated with 4-OHT (Fig 2A,B), indicating effective targeting of *Id2*. These assays confirmed Id2 expression in R837-treated pDCs without 4-OHT exposure (Fig 2A,B). We also observed a 2.3-3.3-fold increase in *Id2* mRNA expression in *Id2*-sufficient pDCs upon treatment with influenza virus, though the data did not reach statistical significance (Fig 2A). We next assessed expression of *Tcf4* mRNA as well as E2-2 target genes. Our data revealed *Tcf4* was downregulated similarly in R837-stimulated CreER and $Id2^{CKO}$ pDCs. By contrast, *Tcf4* was maintained at high amounts in pDCs treated with influenza virus, regardless of genotype (Fig 2C), suggesting differences between R837 and influenza virus-induced TLR7 activation. Moreover, the E2-2 target genes *Irf7, Spib*, and *Tlr9* were upregulated in pDCs treated with influenza compared to non-treated controls and R837-stimulated pDCs (Fig 2D). These results indicate R837 and, to a lesser extent, influenza virus, stimulate *Id2* expression in pDCs. Our results also suggest Id2-independent mechanisms regulate *Tcf4* and E2-2-target gene expression upon TLR7 activation.

3.3. Id2 is largely dispensable for pDC maturation in response to TLR7 stimulation

Prior work using mice with germline deletion of *Id2* indicated Id2 negatively regulates IFN-α production by pDCs (Hacker et al., 2003). To test this in $Id2^{CKO}$ pDCs, and determine whether other pDC-produced cytokines were regulated by Id2, we evaluated protein and mRNA expression. Cytokine and chemokine multiplex assays using pDC culture supernatants revealed R837-stimulated *Id2*-deficient pDCs produced greater amounts of CCL3 and had a trend of reduced IL-6 production compared to *Id2*-sufficient pDCs (Fig 3A,B; Fig S3A). We found IFN-α production was greater in pDCs treated with influenza compared to R837 (Fig 3A,B), however, *Id2*-deficient pDCs produced comparable amounts of IFN-α as well as other proinflammatory factors (Fig 3A,B; Fig S3A). Moreover, *Il6* was reduced upon R837 treatment in *Id2*-deficient pDCs, while similar amounts of *Ccl3*, *Ifna*, and *Tnfa* mRNA were detected in *Id2*-sufficient and -deficient pDCs at baseline or in response to R837; no major differences were detected between genotypes following treatment with influenza (Fig S3B). These data collectively suggest pDC IFN-α production as well as proinflammatory cytokine and chemokine production is largely independent of Id2 following TLR7 activation.

We next tested whether Id2 was required for pDC maturation in response to R837 or influenza virus by analyzing the expression of markers previously associated with *Id2* expression or TLR agonist-induced maturation (Abbas et al., 2020; Ghosh et al., 2010; O'Keeffe et al., 2002). While we observed some distinctions between the expression of these markers in response to R837 versus influenza virus, we did not detect significant differences between *Id2*-sufficient and -deficient pDCs at baseline or following R837 or influenza simulation (Fig 3C; Fig S4). We found MHC-II, the co-stimulatory molecules CD40 and CD86, and the co-inhibitory molecule PD-L1 were induced upon R837 stimulation, while their expression was only modestly affected in pDCs treated with influenza. CCR7 was modestly reduced in response to R837 yet was unaffected in influenza-treated pDCs. By contrast, MHC-I remained unchanged in response to R837 but was induced in influenza-treated pDCs. In addition, pDCs stimulated with R837 upregulated CD8α while expression remained mostly unchanged in response to influenza. Expression of the pan-cDC1 marker XCR1, co-stimulatory marker CD80, DC marker CD11c, and pDC-expressed B220 were unaffected by either treatment. The additional pDC marker Siglec-H was downregulated in response to R837, consistent with prior observations (Puttur et al., 2013), but was retained in response to influenza virus (Fig 3C; Fig S4). Collectively, our data indicate key differences in R837- versus influenza virus-induced pDC maturation responses and suggest Id2 is largely dispensable for these TLR7 agonist-induced phenotypic changes.

3.4. R837 stimulates transcription of *Id2*

Since Id2 is a key factor in DC development, we utilized our pDC culture system to explore mechanisms of *Id2* regulation upon TLR agonist stimulation. Our prior studies demonstrated the *Id2* proximal promoter in pDCs is marked by the modification histone H3 lysine 4 trimethylation (H3K4me3), associated with poised or transcriptionally active genes (Bernstein et al., 2006; Li et al., 2012); yet, it remained unclear whether *Id2* transcription was activated upon TLR agonist treatment. Thus, we employed the transcriptional inhibitor Actinomycin D (AcD) in our pDC culture system. Our results show R837 failed to

induce *Id2* expression in the presence of AcD (Fig 4), suggesting TLR stimulation induces transcriptional activation of *Id2* in pDCs.

We next used the online ConTraV3 tool (Kreft et al., 2017) to screen for the presence of consensus transcription factor binding sites within the *Id2* proximal promoter, which we defined as −5kb upstream of the *Id2* transcriptional start site (TSS, +1). This analysis provided a list of ~450 transcriptional regulators with potential to regulate *Id2*; we subsequently distilled this list based on analysis of a publicly accessible microarray data set providing differentially expressed genes in TLR9 agonist- or influenza-stimulated murine pDCs (GSE7831) (Iparraguirre et al., 2007). Based on overlapping factors from both lists (Fig S5; Table S1), we identified two potential mechanisms of *Id2* regulation mediated by TLR-induced signaling pathways (e.g., Nfkb1 (p50), c-Rel, and AP-1) or by the IFN-α/β receptor (IFNAR) pathway (e.g., STAT1 and STAT2).

3.5. Ubc13 regulates TLR agonist-induced *Id2* expression

To test involvement of TLR agonist-responsive signaling cascades, we used pDCs deficient for Ubc13, which facilitates ubiquitination of lysine 63 on TRAF6 to activate NF-κB and MAP kinase (MAPK) signaling (Deng et al., 2000; Fitzgerald and Kagan, 2020; Fukushima et al., 2007; Hofmann and Pickart, 1999). We generated pDCs from CreER *Ube2n*$^{f/f}$ mice (*Ube2n*^{CKO}) or CreER controls, which enabled 4-OHT-inducible deletion of *Ube2n*/Ubc13 from *Ube2n*^{CKO} cells (Fig 5A). Following R837 stimulation, we found *Ube2n* was upregulated modestly in pDCs, while *Id2* was also induced as expected (Fig 5A,B). Unlike pDCs, *Ube2n* was not induced upon poly I:C or LPS treatment in cDC1s, suggesting induction of *Ube2n* occurs in a cell-intrinsic or agonist-dependent manner (Fig S6A). Additionally, *Ube2n* amounts were expressed similarly or modestly elevated in cDC1s compared to pDCs (Fig S6B). By contrast, R837-responsive expression of *Id2* mRNA was suppressed in 4-OHT-treated *Ube2n*^{CKO} pDCs compared to CreER controls (Fig 5B), implying a role for Ubc13 in *Id2* transcriptional activation. We also detected reduced expression of *Tcf4* in 4-OHT-treated *Ube2n*^{CKO} pDCs but not in *Ube2n*-sufficient pDCs (Fig 5C), suggesting *Ube2n* is important to maintain *Tcf4* expression upon TLR7 agonist stimulation. Furthermore, R837-responsive induction of *Il6, Tnfa*, and *Ifna* was mediated in part by Ubc13, as judged by reduced upregulation in *Ube2n*^{CKO} pDCs (Fig 5D–F). These data are consistent with roles for Ubc13 in promoting TRAF6 activation and TLR-mediated cytokine gene induction (Kawai et al., 2004), and further validate Ubc13-deficiency in *Ube2n*^{CKO} pDCs. *Ube2n*, *Il6,* and *Tnfa* were also modestly reduced in R837-stimulated pDCs from *Ube2n*^{CKO} mice in the absence of 4-OHT (Fig 5A,D,E), suggesting a low amount of Cre activity may be present in the non-4-OHT-containing cultures. Collectively, our data indicate Ubc13 has an important role in mediating the induction of *Id2* as well as key cytokines produced upon TLR7 stimulation in pDCs.

3.6. *Id2* induction is independent of IFNAR signaling

Our results with *Ube2n*^{CKO} pDCs suggested that additional signaling mechanisms control *Id2* induction following R837 stimulation, since *Id2* expression was reduced but not fully suppressed in *Ube2n*-deficient pDCs (Fig 5B). Our *in silico Id2* promoter analysis suggested IFNAR-dependent regulators contribute to *Id2* gene regulation (Table S1). To examine

this, we used pDCs derived from BM of *Ifnar*$^{-/-}$ mice. We confirmed loss of IFNAR signaling by reduction in IFN-α-responsive STAT1 tyrosine phosphorylation (pSTAT1) (Fig 6A). In addition, we found reduced *Irf7* expression in *Ifnar*$^{-/-}$ pDCs relative to *Ifnar*$^{+/+}$ pDCs, while pDCs of both genotypes expressed greater amounts of *Irf7* versus cDC1s, as expected (Fig S7). Moreover, *Ifnar*$^{-/-}$ pDCs failed to upregulate *Irf7* mRNA upon IFN-α or R837 treatment, and demonstrated lower but not significantly reduced *Ifna* expression, indicating loss of autocrine/paracrine IFNAR signaling (Fig 6B). By contrast, our assays showed *Id2* was induced similarly in pDCs from *Ifnar*$^{+/+}$ and *Ifnar*$^{-/-}$ mice upon R837 stimulation (Fig 6B). Collectively, our data indicate *Id2* is regulated in a Ubc13-dependent, IFN-I-independent manner in pDCs following TLR7 agonist stimulation.

4. Discussion

Id and E proteins are critical regulators of immune cell development and function, yet the role of Id2 in DC responses to TLR agonist stimulation has remained unclear. Using pDCs derived from *in vitro* cultures or mice treated with Flt3L HGT, we found TLR7/9 agonists induce Id2 expression. Our data indicate *Id2* is transcriptionally activated upon TLR7 agonist stimulation via a Ubc13-dependent mechanism. Moreover, our results show *Id2* transcriptional activation is independent of IFNAR signaling, ruling out a contribution of autocrine IFN-I signaling in *Id2* gene regulation in pDCs. Regardless, Id2 appears dispensable for pDC maturation, as judged by conditional *Id2* depletion and analysis of canonical phenotypic changes associated with TLR7 agonist-induced maturation responses. Thus, our results suggest Id2-independent mechanisms regulate TLR agonist-induced pDC maturation.

Prior work has demonstrated pDCs that are deficient for the critical lineage regulator E2-2 express increased amounts of *Id2* mRNA and exhibit cDC-like features (Ghosh et al., 2010). Additional studies have reported reduction of *Tcf4* or inverse expression of *Tcf4* and *Id2* in TLR agonist-, CD40L-, or virus-activated pDCs (Abbas et al., 2020; Alcántara-Hernández et al., 2017; Cisse et al., 2008; Leylek et al., 2020; Macal et al., 2018). Moreover, E2-2 is required for IFN-α secretion from pDCs (Cisse et al., 2008), while Id2 has been implicated in suppression of IFN-α production upon viral exposure (Hacker et al., 2003). These data collectively suggested that induction of Id2 during pDC maturation may suppress E2-2 activity, dampen IFN-α production, and enable pDCs to acquire cDC-like features. We found concomitant induction of Id2 and suppression of E2-2 in R837-stimulated pDCs. Nonetheless, our studies with conditional *Id2* deletion from pDCs failed to support a key role for Id2 in TLR agonist-induced suppression of *Tcf4* or E2-2 target gene expression. Taken together, our data suggest that reduction in the expression of E2-2 rather than induction of Id2 promotes pDC maturation upon R837 treatment. Thus, additional efforts to delineate mechanisms regulating *Tcf4* in response to TLR agonists are important for fundamental understanding of pDC biology.

IFNAR signaling was shown to repress *Tcf4* expression in BM pDC progenitors (Macal et al., 2018); however, in agreement with recent findings from others (Dewald et al., 2020), we did not find evidence for involvement of IFNAR in mediating *Tcf4* inhibition in pDCs upon TLR7 stimulation (data not shown). As these data suggested alternate pathways regulate

Tcf4 downregulation in response to TLR7 agonists, we also assessed the role of Ubc13. Our data indicated *Tcf4* was reduced in *Ube2n*-deficient pDCs, suggesting that Ubc13 may be required to maintain *Tcf4* expression in TLR7 agonist-stimulated pDCs.

Although R837 and influenza are ligands for TLR7, we found pDCs produced abundant amounts of IFN-α yet lower amounts of pro-inflammatory factors after treatment with influenza versus R837. A prior study using human pDCs stimulated with R837 or influenza virus found delayed kinetics of NF-κB-dependent CCL3 production from influenza-treated pDCs, while the kinetics of TNF-α production were comparable between the treatments (Lo et al., 2012). Similarly, we found R837 promoted strong upregulation of MHC-II, co-stimulatory molecules CD40 and CD86, co-inhibitory molecule PD-L1, and CD8α compared to pDCs treated with influenza virus, while MHC-I was induced and CCR7 and Siglec-H were retained in pDCs only upon influenza treatment, indicating the ligands differentially affect pDC cell surface maturation. These results suggest differences in ligand internalization and transit or residence within specific endosomal compartments may contribute to the distinct pDC maturation kinetics observed. To our knowledge, no studies have directly compared endosomal signaling between these two ligands. This may be an important area for future investigation to better understand pDC biology in response to various TLR ligands.

pDC-mediated IFN-I responses are important during certain viral infections (Cervantes-Barragan et al., 2012; Chopin et al., 2016; Wang et al., 2012), yet the mechanisms regulating pDC IFN-I production as well as other proinflammatory factors are not fully defined. *Id2*$^{-/-}$ murine pDCs were previously shown to produce elevated IFN-α after stimulation with influenza- or herpes simplex viruses (Hacker et al., 2003). While we were unable to replicate these findings with R837 or heat-inactivated influenza virus, our cytokine production assays suggest Id2 modestly regulates CCL3 and IL-6 production following R837 treatment *in vitro*. CCL3 and IL-6 promote immune cell recruitment or adaptive immune cell activation and differentiation, indicating Id2 may affect pDC-mediated responses. Additionally, little is known about Ubc13 roles in pDC maturation and antiviral immunity. We observed induction of *Ube2n* in response to R837 stimulation in pDCs that was not observed in TLR3 or TLR4 agonist-stimulated cDC1s. Our data with conditional *Ube2n* deletion revealed Ubc13 was required for optimal induction of *Ifna*, *Il6*, and *Tnfa* in pDCs treated with R837, but did not affect cDC1 induction of *Il6*. While beyond the scope of our study, future work should consider evaluating the functional relevance of both Id2 and Ubc13 in pDC-mediated cytokine responses and immune cell recruitment and status during viral infection.

Importantly, we utilized pDC purification methods that were designed to exclude lymphoid lineages (i.e., B cells, T cells, NK cells), as well as cDCs. We also confirmed the identity of the pDCs utilized in our study, and ruled out effects from contaminating subsets by treating purified pDCs with agonists for TLR3 or TLR4, which are not enriched in pDCs (Heng et al., 2008), or with GM-CSF, which was shown to differentiate CCR9^{lo} BM pDC precursors into cDCs (Schlitzer et al., 2011). Analysis by flow cytometry revealed minimal changes in pDC cell surface markers upon TLR3 or TLR4 agonist treatment or GM-CSF exposure, compared to non-treated pDCs (data not shown), indicating a lack of response to these stimuli. Furthermore, the cell surface phenotype of stimulated and non-stimulated pDCs was

distinct from purified cDC1s used as controls (data not shown). These findings indicate that our purified pDC population was highly enriched and excluded major contaminating populations including cDCs.

Id2 is a critical regulator of DC development, and also directs diverse biological processes including development and differentiation of immune and non-immune cells (Kee, 2009; Murre, 2019). Cytokines such as IL-2, IL-12, GM-CSF, LIF, and IL-21 induce *Id2* gene expression in T cells and DCs (Yang et al., 2011) (Li et al., 2012) (Sesti-Costa et al., 2020); yet, the mechanisms stimulating *Id2* gene expression in TLR agonist-stimulated pDCs remained unclear. Our investigation focused on TLR-responsive and IFNAR pathways, based on our *in silico* analyses of putative *Id2* regulators. We found Ubc13 but not IFNAR signaling controls *Id2* expression in pDCs treated with the TLR7 agonist R837. Notably, Ubc13 regulates NF-κB as well as MAPK signaling pathways, which are induced downstream of TLR activation (Iparraguirre et al., 2007). Our *in silico* studies predict sites for AP-1 and NF-κB in the *Id2* promoter, suggesting one or more Ubc13-controlled pathways directly stimulate *Id2* transcription. Importantly, other receptors such as IL-1R, CD40, TCR, and BCR utilize TRAF6 and Ubc13 (Hodge et al., 2016; Yamamoto et al., 2006). Thus, our data suggests a role for Ubc13 in *Id2* induction by CD40L-CD40 signaling in pDCs (Leylek et al., 2020). Moreover, our results may be relevant to non-DC lineages. For instance, Id2 induction in response to TCR signaling mediates $CD4^+$ and $CD8^+$ T cell differentiation, effector function, or memory formation (Cannarile et al., 2006; Omilusik et al., 2018; Shaw et al., 2016). In addition, IL-1β promotes *Id2* expression in T regulatory cells, and enhances conversion of T regulatory cells to a T helper 17 phenotype (Hwang et al., 2018). Collectively, the results suggest Ubc13-mediated control of Id2 may contribute to key adaptive immune responses while it is dispensable for pDC maturation.

5. Conclusions

We investigated mechanisms by which TLR agonists stimulate *Id2* expression in pDCs and potential roles for Id2 in pDC maturation. We found TLR7 agonist-responsive Id2 expression in pDCs requires Ubc13 but is independent of IFNAR signaling, indicating TLR-induced signaling pathways directly stimulate *Id2* gene activity. Additionally, while we found Id2 was upregulated upon TLR7 agonist treatment, it appears to be largely dispensable for pDC maturation. Collectively, our results implicate new pathways in *Id2* gene regulation and indicate Id2-independent mechanisms control pDC maturation.

Supplementary Material

Refer to Web version on PubMed Central for supplementary material.

Acknowledgments

We thank Dr. Haiyan Li for advice and guidance on DC cultures; Dr. Anna Lasorella and Dr. Barbara Kee for generously providing the *Id2*-floxed mice; Dr. Kylee Veazey and Dr. Margarida Santos for helpful advice; and the MD Anderson South Campus Flow Cytometry Core Facility for experimental assistance.

Funding

This work was supported by the NIH NIAID (R01AI109294 and R01AI133822 to S.S.W.), the Cancer Prevention and Research Institute of Texas (CPRIT) Research Training award (RP170067 to R.L.B. and T.T.C., and RP210028 to L.M.K.); and the MD Anderson Cancer Center Core grant from NIH NCI (P30CA016672; supporting the MD Anderson South Campus Flow Cytometry Core Facility)

Abbreviations:

4-OHT	4-hydroxytamoxifen
AcD	Actinomycin D
ANOVA	analysis of variance
β-ME	β-mercaptoethanol
BM	bone marrow
CD40L	CD40 ligand
cDC1	type 1 conventional dendritic cell
cDC2	type 2 conventional dendritic cell
CCL-	CC motif chemokine ligand
CXCL-	C-X-C motif chemokine ligand
DC	dendritic cell
FACS	fluorescence-activated cell sorting
FCS	fetal calf serum
Flt3	FMS-like tyrosine kinase 3
flu	influenza virus
G-CSF	granulocyte colony-stimulating factor
GM-CSF	granulocyte-macrophage colony-stimulating factor
HLH	helix-loop-helix
HGT	hydrodynamic gene transfer
Id2	inhibitor of DNA binding 2
IFN-I	type I IFN
IFNAR	IFN- α/β receptor
IL-	interleukin
LIF	leukemia inhibitory factor
Lin	lineage

LPS	lipopolysaccharide
LSB	Laemmli sample buffer
M-CSF	macrophage colony-stimulating factor
MFI	mean fluorescence intensity
MHC-II	major histocompatibility complex class II
PBS	phosphate-buffered saline
pDC	plasmacytoid dendritic cell
qRT-PCR	quantitative RT-PCR
R837	Imiquimod
RPMI	Roswell Park Memorial Institute
RT	room temperature
SEM	standard error of the mean
TBST	Tris-buffered saline containing Tween-20
TLR	Toll-like receptor
TNF-α	tumor necrosis factor alpha

References

Abbas A, Vu Manh TP, Valente M, Collinet N, Attaf N, Dong C, Naciri K, Chelbi R, Brelurut G, Cervera-Marzal I, Rauwel B, Davignon JL, Bessou G, Thomas-Chollier M, Thieffry D, Villani AC, Milpied P, Dalod M, Tomasello E, 2020. The activation trajectory of plasmacytoid dendritic cells in vivo during a viral infection. Nat. Immunol 21, 983–997. 10.1038/s41590-020-0731-4 [PubMed: 32690951]

Alcántara-Hernández M, Leylek R, Wagar LE, Engleman EG, Keler T, Marinkovich MP, Davis MM, Nolan GP, Idoyaga J, 2017. High-Dimensional Phenotypic Mapping of Human Dendritic Cells Reveals Interindividual Variation and Tissue Specialization. Immunity 47, 1037–1050.e6. 10.1016/j.immuni.2017.11.001 [PubMed: 29221729]

Asselin-Paturel C, Boonstra A, Dalod M, Durand I, Yessaad N, Dezutter-Dambuyant C, Vicari A, O'Garra A, Biron C, Brière F, Trinchieri G, 2001. Mouse type I IFN-producing cells are immature APCs with plasmacytoid morphology. Nat. Immunol 2, 1144–1150. 10.1038/ni736 [PubMed: 11713464]

Asselin-Paturel C, Brizard G, Chemin K, Boonstra A, O'Garra A, Vicari A, Trinchieri G, 2005. Type I interferon dependence of plasmacytoid dendritic cell activation and migration. J. Exp. Med. 201, 1157–1167. 10.1084/jem.20041930 [PubMed: 15795237]

Bagadia P, Huang X, Liu T-T, Durai V, Grajales-Reyes GE, Nitschké M, Modrusan Z, Granja JM, Satpathy AT, Briseño CG, Gargaro M, Iwata A, Kim S, Chang HY, Shaw AS, Murphy TL, Murphy KM, 2019. An Nfil3–Zeb2–Id2 pathway imposes Irf8 enhancer switching during cDC1 development. Nat. Immunol. 20, 1174–1185. 10.1038/s41590-019-0449-3 [PubMed: 31406377]

Benezra R, Davis RL, Lockshon D, Turner DL, Weintraub H, 1990. The Protein Id: A Negative Regulator of Helix-Loop-Helix DNA Binding Proteins. Cell 61, 49–59. 10.1016/0092-8674(90)90214-Y [PubMed: 2156629]

Bernstein BE, Mikkelsen TS, Xie X, Kamal M, Huebert DJ, Cuff J, Fry B, Meissner A, Wernig M, Plath K, Jaenisch R, Wagschal A, Feil R, Schreiber SL, Lander ES, 2006. A Bivalent Chromatin Structure Marks Key Developmental Genes in Embryonic Stem Cells. Cell 125, 315–326. 10.1016/j.cell.2006.02.041 [PubMed: 16630819]

Böttcher JP, Reis e Sousa C, 2018. The Role of Type 1 Conventional Dendritic Cells in Cancer Immunity. Trends in Cancer 4, 784–792. 10.1016/j.trecan.2018.09.001 [PubMed: 30352680]

Cannarile MA, Lind NA, Rivera R, Sheridan AD, Camfield KA, Wu BB, Cheung KP, Ding Z, Goldrath AW, 2006. Transcriptional regulator Id2 mediates CD8+ T cell immunity. Nat. Immunol. 7, 1317–1325. 10.1038/ni1403 [PubMed: 17086188]

Cella M, Jarrossay D, Facchetti F, Alebardi O, Nakajima H, Lanzavecchia A, Colonna M, 1999. Plasmacytoid monocytes migrate to inflamed lymph nodes and produce large amounts of type I interferon. Nat. Med. 5, 919–923. 10.1038/11360 [PubMed: 10426316]

Cervantes-Barragan L, Lewis KL, Firner S, Thiel V, Hugues S, Reith W, Ludewig B, Reizis B, 2012. Plasmacytoid dendritic cells control T-cell response to chronic viral infection. Proc. Natl. Acad. Sci. U. S. A. 109, 3012–3017. 10.1073/pnas.1117359109 [PubMed: 22315415]

Chopin M, Preston SP, Lun ATL, Tellier J, Smyth GK, Pellegrini M, Belz GT, Corcoran LM, Visvader JE, Wu L, Nutt SL, 2016. RUNX2 Mediates Plasmacytoid Dendritic Cell Egress from the Bone Marrow and Controls Viral Immunity. Cell Rep. 15, 866–878. 10.1016/j.celrep.2016.03.066 [PubMed: 27149837]

Chrisikos TT, Zhou Y, Li HS, Babcock RL, Wan X, Patel B, Newton K, Mancuso JJ, Watowich SS, 2020. STAT3 Inhibits CD103+ cDC1 Vaccine Efficacy in Murine Breast Cancer. Cancers (Basel). 12, 128. 10.3390/cancers12010128 [PubMed: 31947933]

Chrisikos TT, Zhou Y, Slone N, Babcock R, Watowich SS, Li HS, 2019. Molecular regulation of dendritic cell development and function in homeostasis, inflammation, and cancer. Mol. Immunol. 110, 24–39. 10.1016/j.molimm.2018.01.014 [PubMed: 29549977]

Church GM, Ephrussi A, Gilbert W, Tonegawa S, 1985. Cell-type-specific contacts to immunoglobulin enhancers in nuclei. Nature 313, 798–801. 10.1038/313798a0 [PubMed: 3919308]

Cisse B, Caton ML, Lehner M, Maeda T, Scheu S, Locksley R, Holmberg D, Zweier C, den Hollander NS, Kant SG, Holter W, Rauch A, Zhuang Y, Reizis B, 2008. Transcription Factor E2-2 Is an Essential and Specific Regulator of Plasmacytoid Dendritic Cell Development. Cell 135, 37–48. 10.1016/j.cell.2008.09.016 [PubMed: 18854153]

Deng L, Wang C, Spencer E, Yang L, Braun A, You J, Slaughter C, Pickart C, Chen ZJ, 2000. Activation of the Iκb kinase complex by TRAF6 requires a dimeric ubiquitin-conjugating enzyme complex and a unique polyubiquitin chain. Cell 103, 351–361. 10.1016/S0092-8674(00)00126-4 [PubMed: 11057907]

Dewald HK, Hurley HJ, Fitzgerald-Bocarsly P, 2020. Regulation of Transcription Factor E2-2 in Human Plasmacytoid Dendritic Cells by Monocyte-Derived TNFα. Viruses 12, 162. 10.3390/v12020162 [PubMed: 32023836]

Ephrussi A, Church GM, Tonegawa S, Gilbert W, 1985. B Lineage-Specific Interactions of an Immunoglobulin Enhancer with Cellular Factors in Vivo. Science 227, 134–140. 10.1126/science.3917574 [PubMed: 3917574]

Fitzgerald KA, Kagan JC, 2020. Toll-like Receptors and the Control of Immunity. Cell 180, 1044–1066. 10.1016/j.cell.2020.02.041 [PubMed: 32164908]

Fukushima T, Matsuzawa SI, Kress CL, Bruey JM, Krajewska M, Lefebvre S, Zapata JM, Ronai Z, Reed JC, 2007. Ubiquitin-conjugating enzyme Ubc13 is a critical component of TNF receptor-associated factor (TRAF)-mediated inflammatory responses. Proc. Natl. Acad. Sci. U. S. A. 104, 6371–6376. 10.1073/pnas.0700548104 [PubMed: 17404240]

Ghosh HS, Ceribelli M, Matos I, Lazarovici A, Bussemaker HJ, Lasorella A, Hiebert SW, Liu K, Staudt LM, Reizis B, 2014. ETO family protein Mtg16 regulates the balance of dendritic cell subsets by repressing Id2. J. Exp. Med. 211, 1623–1635. 10.1084/jem.20132121 [PubMed: 24980046]

Ghosh HS, Cisse B, Bunin A, Lewis KL, Reizis B, 2010. Continuous Expression of the Transcription Factor E2–2 Maintains the Cell Fate of Mature Plasmacytoid Dendritic Cells. Immunity 33, 905–916. 10.1016/j.immuni.2010.11.023 [PubMed: 21145760]

Grajkowska LT, Ceribelli M, Lau CM, Warren ME, Tiniakou I, Nakandakari Higa S, Bunin A, Haecker H, Mirny LA, Staudt LM, Reizis B, 2017. Isoform-Specific Expression and Feedback Regulation of E Protein TCF4 Control Dendritic Cell Lineage Specification. Immunity 46, 65–77. 10.1016/j.immuni.2016.11.006 [PubMed: 27986456]

Guilliams M, Ginhoux F, Jakubzick C, Naik SH, Onai N, Schraml BU, Segura E, Tussiwand R, Yona S, 2014. Dendritic cells, monocytes and macrophages: A unified nomenclature based on ontogeny. Nat. Rev. Immunol. 14, 571–578. 10.1038/nri3712 [PubMed: 25033907]

Hacker C, Kirsch RD, Ju X-S, Hieronymus T, Gust TC, Kuhl C, Jorgas T, Kurz SM, Rose-John S, Yokota Y, Zenke M, 2003. Transcriptional profiling identifies Id2 function in dendritic cell development. Nat. Immunol. 4, 380–386. 10.1038/ni903 [PubMed: 12598895]

Heng TSP, Painter MW, The Immunological Genome Project Consortium, 2008. The Immunological Genome Project: networks of gene expression in immune cells. Nat. Immunol. 9, 1091–1094. 10.1038/ni1008-1091 [PubMed: 18800157]

Hilligan KL, Ronchese F, 2020. Antigen presentation by dendritic cells and their instruction of CD4+ T helper cell responses. Cell. Mol. Immunol. 17, 587–599. 10.1038/s41423-020-0465-0 [PubMed: 32433540]

Hodge CD, Spyracopoulos L, Mark Glover JN, 2016. Ubc13: The Lys63 ubiquitin chain building machine. Oncotarget 7, 64471–64504. 10.18632/oncotarget.10948 [PubMed: 27486774]

Hofmann RM, Pickart CM, 1999. Noncanonical MMS2-Encoded Ubiquitin-Conjugating Enzyme Functions in Assembly of Novel Polyubiquitin Chains for DNA Repair. Cell 96, 645–653. 10.1016/s0092-8674(00)80575-9 [PubMed: 10089880]

Honda K, Yanai H, Negishi H, Asagiri M, Sato M, Mizutani T, Shimada N, Ohba Y, Takaoka A, Yoshida N, Taniguchi T, 2005. IRF-7 is the master regulator of type-I interferon-dependent immune responses. Nature 434, 772–777. 10.1038/nature03419.1. [PubMed: 15800576]

Hwang SM, Sharma G, Verma R, Byun S, Rudra D, Im SH, 2018. Inflammation-induced Id2 promotes plasticity in regulatory T cells. Nat. Commun. 9, 1–13. 10.1038/s41467-018-07254-2 [PubMed: 29317637]

Iparraguirre A, Tobias JW, Hensley SE, Masek KS, Cavanagh LL, Rendl M, Hunter CA, Ertl HC, von Andrian UH, Weninger W, 2007. Two distinct activation states of plasmacytoid dendritic cells induced by influenza virus and CpG 1826 oligonucleotide. J. Leukoc. Biol. 83, 610–620. 10.1189/jlb.0807511 [PubMed: 18029397]

Kawai T, Sato S, Ishii KJ, Coban C, Hemmi H, Yamamoto M, Terai K, Matsuda M, Inoue JI, Uematsu S, Takeuchi O, Akira S, 2004. Interferon-α induction through Toll-like receptors involves a direct interaction of IRF7 with MyD88 and TRAF6. Nat. Immunol. 5, 1061–1068. 10.1038/ni1118 [PubMed: 15361868]

Kawasaki T, Kawai T, 2014. Toll-like receptor signaling pathways. Front. Immunol. 5, 1–8. 10.3389/fimmu.2014.00461 [PubMed: 24474949]

Kee BL, 2009. E and ID proteins branch out. Nat. Rev. Immunol. 9, 175–184. 10.1038/nri2507 [PubMed: 19240756]

Kreft L, Soete A, Hulpiau P, Botzki A, Saeys Y, De Bleser P, 2017. ConTra v3: a tool to identify transcription factor binding sites across species, update 2017. Nucleic Acids Res. 45, W490–W494. 10.1093/nar/gkx376 [PubMed: 28472390]

Leylek R, Alcántara-Hernández M, Granja JM, Chavez M, Perez K, Diaz OR, Li R, Satpathy AT, Chang HY, Idoyaga J, 2020. Chromatin Landscape Underpinning Human Dendritic Cell Heterogeneity. Cell Rep. 32, 103180. 10.1016/j.celrep.2020.108180

Li HS, Yang CY, Nallaparaju KC, Zhang H, Liu YJ, Goldrath AW, Watowich SS, 2012. The signal transducers STAT5 and STAT3 control expression of Id2 and E2–2 during dendritic cell development. Blood 120, 4363–4373. 10.1182/blood-2012-07-441311 [PubMed: 23033267]

Liu C, Wang G, Hwu P, Liu C, Lou Y, Lizée G, Qin H, Liu S, Rabinovich B, Liu Y, Wang G, Hwu P, 2008. Plasmacytoid dendritic cells induce NK cell-dependent, tumor antigen-specific T cell cross-priming and tumor regression in mice. J. Clin. Invest. 118, 1165–1175. 10.1172/JCI33583.as [PubMed: 18259609]

Liu F, Song YK, Liu D, 1999. Hydrodynamics-based transfection in animals by systemic administration of plasmid DNA. Gene Ther. 6, 1258–1266. 10.1038/sj.gt.3300947 [PubMed: 10455434]

Lo CC, Schwartz JA, Johnson DJ, Yu M, Aidarus N, Mujib S, Benko E, Hyrcza M, Kovacs C, Ostrowski MA, 2012. HIV Delays IFN-α Production from Human Plasmacytoid Dendritic Cells and Is Associated with SYK Phosphorylation. PLoS One 7, 1–11. 10.1371/journal.pone.0037052

Macal M, Jo Y, Dallari S, Chang AY, Dai J, Swaminathan S, Wehrens EJ, Fitzgerald-Bocarsly P, Zúñiga EI, 2018. Self-Renewal and Toll-like Receptor Signaling Sustain Exhausted Plasmacytoid Dendritic Cells during Chronic Viral Infection. Immunity 48, 730–744.e5. 10.1016/j.immuni.2018.03.020 [PubMed: 29669251]

Mouriès J, Moron G, Schlecht G, Escriou N, Dadaglio G, Lederc C, 2008. Plasmacytoid dendritic cells efficiently cross-prime naive T cells in vivo after TLR activation. Blood 112, 3713–3722. 10.1182/blood-2008-03-146290 [PubMed: 18698004]

Müller U, Steinhoff U, Reis LFL, Hemmi S, Pavlovic J, Zinkernagel RM, Aguet M, 1994. Functional Role of Type I and Type II Interferons in Antiviral Defense. Science 264, 1918–1921. 10.1126/science.8009221 [PubMed: 8009221]

Murre C, 2019. Helix–loop–helix proteins and the advent of cellular diversity: 30 years of discovery. Genes Dev. 33, 6–25. 10.1101/gad.320663.118 [PubMed: 30602438]

Murre C, McCaw PS, Baltimore D, 1989a. A New DNA Binding and Dimerization Motif in lmmunoglobulin Enhancer Binding, daughterless, MyoD, myc Proteins. Cell 56, 777–783. 10.1016/0092-8674(89)90682-x [PubMed: 2493990]

Murre C, McCaw PS, Vaessin H, Caudy M, Jan LY, Jan YN, Cabrera CV, Buskin JN, Hauschka SD, Lassar AB, Weintraub H, Baltimore D, 1989b. Interactions between Heterologous Helix-Loop-Helix Proteins Generate Complexes That Bind Specifically to a Common DNA Sequence. Cell 58, 537–544. 10.1016/0092-8674(89)90434-0 [PubMed: 2503252]

Nagasawa M, Schmidlin H, Hazekamp MG, Schotte R, Blom B, 2008. Development of human plasmacytoid dendritic cells depends on the combined action of the basic helix-loop-helix factor E2-2 and the Ets factor Spi-B. Eur. J. Immunol. 38, 2389–2400. 10.1002/eji.200838470 [PubMed: 18792017]

Niola F, Zhao X, Singh D, Castano A, Sullivan R, Lauria M, Nam HS, Zhuang Y, Benezra R, Di Bernardo D, Iavarone A, Lasorella A, 2012. Id proteins synchronize stemness and anchorage to the niche of neural stem cells. Nat. Cell Biol. 14, 477–487. 10.1038/ncb2490 [PubMed: 22522171]

O'Keeffe M, Hochrein H, Vremec D, Caminschi I, Miller JL, Anders EM, Wu L, Lahoud MH, Henri S, Scott B, Hertzog P, Tatarczuch L, Shortman K, 2002. Mouse Plasmacytoid Cells: Long-lived Cells, Heterogeneous in Surface Phenotype and Function, that Differentiate Into CD8+ Dendritic Cells Only after Microbial Stimulus. J. Exp. Med. 196, 1307–1319. 10.1084/jem.20021031 [PubMed: 12438422]

Omilusik KD, Nadjsombati MS, Shaw LA, Yu B, Milner JJ, Goldrath AW, 2018. Sustained Id2 regulation of E proteins is required for terminal differentiation of effector CD8+ T cells. J. Exp. Med. 215, 773–783. 10.1084/jem.20171584 [PubMed: 29440362]

Puttur F, Arnold-Schrauf C, Lahl K, Solmaz G, Lindenberg M, Mayer CT, Gohmert M, Swallow M, van Helt C, Schmitt H, Nitschke L, Lambrecht BN, Lang R, Messerle M, Sparwasser T, 2013. Absence of Siglec-H in MCMV Infection Elevates Interferon Alpha Production but Does Not Enhance Viral Clearance. PLoS Pathog. 9, e1003648. 10.1371/journal.ppat.1003648 [PubMed: 24086137]

Reizis B, 2019. Plasmacytoid Dendritic Cells: Development, Regulation, and Function. Immunity 50, 37–50. 10.1016/j.immuni.2018.12.027 [PubMed: 30650380]

Robert L,D, Pei-Feng C, Lassar B,A, Harold W, 1990. The MyoD DNA Binding Domain Contains a Recognition Code for Muscle-Specific Gene Activation. Cell 60, 733–746. 10.1016/0092-8674(90)90088-v [PubMed: 2155707]

Salio M, Palmowski MJ, Atzberger A, Hermans IF, Cerundolo V, 2004. CpG-matured Murine Plasmacytoid Dendritic Cells Are Capable of In Vivo Priming of Functional CD8 T Cell Responses to Endogenous but Not Exogenous Antigens. J. Exp. Med. 199, 567–579. 10.1084/jem.20031059 [PubMed: 14970182]

Schlecht G, Garcia S, Escriou N, Freitas AA, Leclerc C, Dadaglio G, 2004. Murine plasmacytoid dendritic cells induce effector/memory CD8+ T-cell responses in vivo after viral stimulation. Blood 104, 1808–1815. 10.1182/blood-2004-02-0426 [PubMed: 15166034]

Schlitzer A, Loschko J, Mair K, Vogelmann R, Henkel L, Einwächter H, Schiemann M, Niess JH, Reindl W, Krug A, 2011. Identification of CCR9- murine plasmacytoid DC precursors with plasticity to differentiate into conventional DCs. Blood 117, 6562–6570. 10.1182/blood-2010-12-326678 [PubMed: 21508410]

Sesti-Costa R, Cervantes-Barragan L, Swiecki MK, Fachi JL, Cella M, Gilfillan S, Silva JS, Colonna M, 2020. Leukemia Inhibitory Factor Inhibits Plasmacytoid Dendritic Cell Function and Development. J. Immunol. 204, 2257–2268. 10.4049/jimmunol.1900604 [PubMed: 32169845]

Shaw LA, Bélanger S, Omilusik KD, Cho S, Scott-Browne JP, Nance JP, Goulding J, Lasorella A, Lu LF, Crotty S, Goldrath AW, 2016. Id2 reinforces TH 1 differentiation and inhibits E2A to repress TFH differentiation. Nat. Immunol. 17, 834–843. 10.1038/ni.3461 [PubMed: 27213691]

Siegal FP, Kadowaki N, Shodell M, Fitzgerald-Bocarsly PA, Shah K, Ho S, Antonenko S, Liu YJ, 1999. The Nature of the Principal Type 1 Interferon-Producing Cells in Human Blood. Science 284, 1835–1837. 10.1126/science.284.5421.1835 [PubMed: 10364556]

Spits H, Couwenberg F, Bakker AQ, Weijer K, Uittenbogaart CH, 2000. Id2 and Id3 Inhibit Development of CD34+ Stem Cells into Predendritic Cell (Pre-DC)2 but Not into Pre-DC1: Evidence for a Lymphoid Origin of Pre-DC2. J Exp Med 192, 1775–1784. 10.1084/jem.192.12.1775 [PubMed: 11120774]

Steinman RM, Cohn ZA, 1973. Identification of a novel cell type in periperhal lymphoid organs of mice. I. Morphology, quantitation, tissue distribution. J. Exp. Med. 137, 1142–1162. 10.1084/jem.137.5.1142 [PubMed: 4573839]

Swiecki M, Colonna M, 2015. The multifaceted biology of plasmacytoid dendritic cells. Nat. Rev. Immunol. 15, 471–485. 10.1038/nri3865 [PubMed: 26160613]

Tomasello E, Naciri K, Chelbi R, Bessou G, Fries A, Gressier E, Abbas A, Pollet E, Pierre P, Lawrence T, Vu Manh T, Dalod M, 2018. Molecular dissection of plasmacytoid dendritic cell activation in vivo during a viral infection. EMBO J. 37, 1–19. 10.15252/embj.201798836 [PubMed: 29212815]

Ventura A, Kirsch DG, McLaughlin ME, Tuveson DA, Grimm J, Lintault L, Newman J, Reczek EE, Weissleder R, Jacks T, 2007. Restoration of p53 function leads to tumour regression in vivo. Nature 445, 661–665. 10.1038/nature05541 [PubMed: 17251932]

Wang Y, Swiecki M, Cella M, Alber G, Schreiber RD, Gilfillan S, Colonna M, 2012. Timing and magnitude of type i interferon responses by distinct sensors impact CD8 T cell exhaustion and chronic viral infection. Cell Host Microbe 11, 631–642. 10.1016/j.chom.2012.05.003 [PubMed: 22704623]

Wimmers F, Subedi N, van Buuringen N, Heister D, Vivié J, Beeren-Reinieren I, Woestenenk R, Dolstra H, Piruska A, Jacobs JFM, van Oudenaarden A, Figdor CG, Huck WTS, de Vries IJM, Tel J, 2018. Single-cell analysis reveals that stochasticity and paracrine signaling control interferon-alpha production by plasmacytoid dendritic cells. Nat. Commun. 9, 1–12. 10.1038/s41467-018-05784-3 [PubMed: 29317637]

Wu J, Li S, Yang Y, Zhu S, Zhang M, Qiao Y, Liu YJ, Chen J, 2017. TLR-activated plasmacytoid dendritic cells inhibit breast cancer cell growth in vitro and in vivo. Oncotarget 8, 11708–11718. 10.18632/oncotarget.14315 [PubMed: 28052019]

Yamamoto M, Okamoto T, Takeda K, Sato S, Sanjo H, Uematsu S, Saitoh T, Yamamoto N, Sakurai H, Ishii KJ, Yamaoka S, Kawai T, Matsuura Y, Takeuchi O, Akira S, 2006. Key function for the Ubc13 E2 ubiquitin-conjugating enzyme in immune receptor signaling. Nat. Immunol. 7, 962–970. 10.1038/ni1367 [PubMed: 16862162]

Yang CY, Best JA, Knell J, Yang E, Sheridan AD, Jesionek AK, Li HS, Rivera RR, Lind KC, D'Cruz LM, Watowich SS, Murre C, Goldrath AW, 2011. The transcriptional regulators Id2 and Id3 control the formation of distinct memory CD8+ T cell subsets. Nat. Immunol. 12, 1221–1229. 10.1038/ni.2158 [PubMed: 22057289]

Zhou Y, Slone N, Chrisikos TT, Kyrysyuk O, Babcock RL, Medik YB, Li HS, Kleinerman ES, Watowich SS, 2020. Vaccine efficacy against primary and metastatic cancer with in vitro-generated CD103+ conventional dendritic cells. J. Immunother. Cancer 8, e000474. 10.1136/jitc-2019-000474 [PubMed: 32273347]

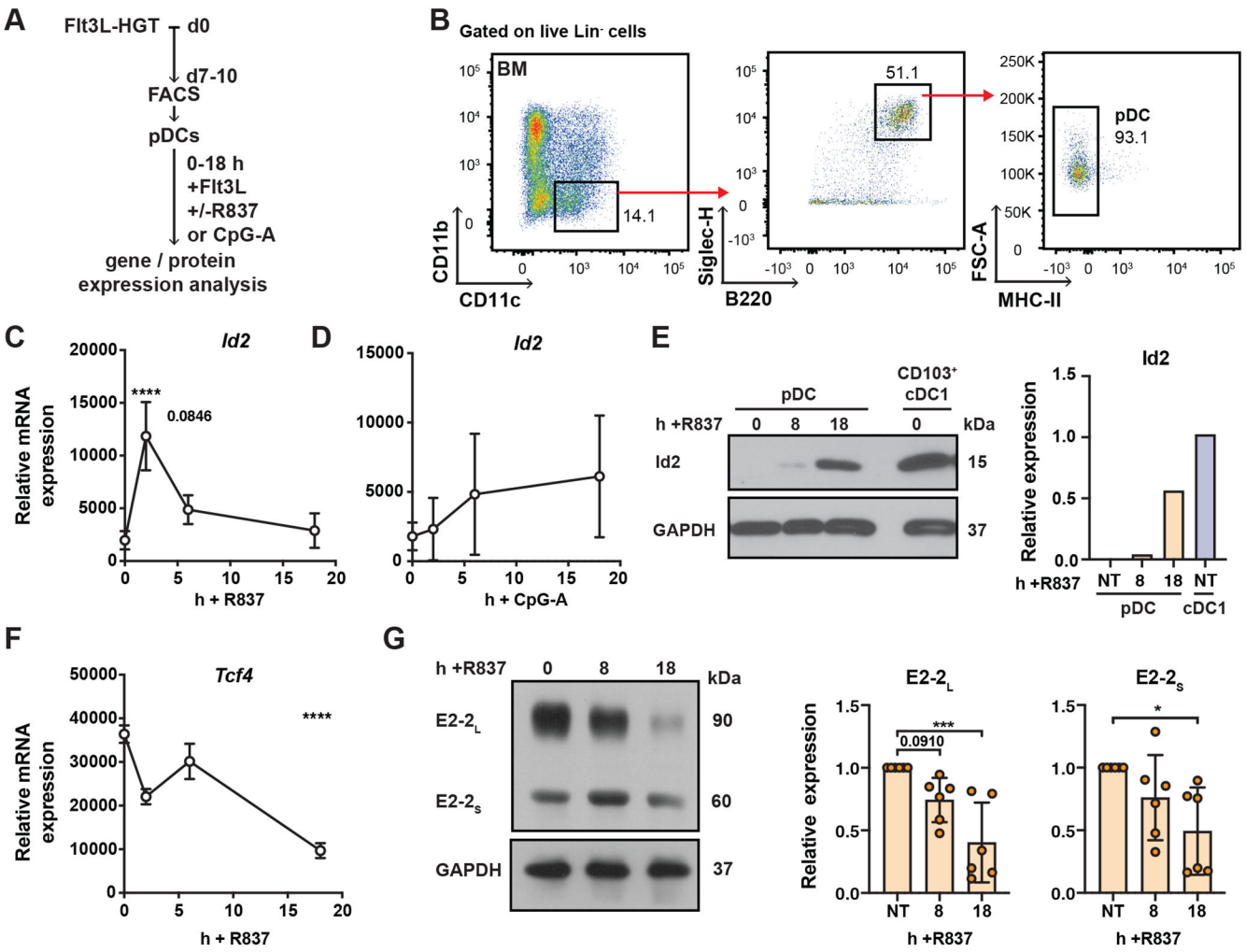

Figure 1: Id2 and E2-2 expression in R837-stimulated pDCs.

(A) Experimental overview of Flt3L-hydrodynamic gene transfer (HGT) treatment in mice followed by purification of pDCs by FACS, and subsequent pDC stimulation with or without R837 (5 μg/mL) or CpG-A (1 μM). (B) Representative gating strategy to purify pDCs by FACS. (C,D) *Id2* mRNA expression in BM pDCs from C57BL/6J mice, following stimulation *in vitro* with R837 (C) or CpG-A (D) for 0, 2, 6, or 18 h, in the presence of Flt3L (50 ng/mL). *Id2* mRNA normalized to *Rpl13* (C,D). (E) Representative immunoblot (left) of whole cell lysates from pDCs and CD103$^+$ cDC1s derived from cultures *in vitro*. pDCs were stimulated with R837 for 0, 8, or 18 h in the presence of Flt3L. Id2 and GAPDH were detected by antibody staining. Id2 expression normalized to GAPDH. (F) *Tcf4* mRNA expression in splenic pDCs, following stimulation *in vitro* with R837 for 0, 2, 6, or 18 h in the presence of Flt3L. *Tcf4* mRNA normalized to *Rpl13*. (G) Representative immunoblot (left) of whole cell lysates from pDCs, treated for the indicated times (h) with R837 in the presence of Flt3L. E2-2 and GAPDH were detected by antibody staining; expression of E2-2$_L$ and E2-2$_S$ (E2-2 long and short isoforms, respectively) normalized to GAPDH (right). Blots were adjusted for brightness equally across the image, and were cropped to show protein bands (E,G). Data shown as mean ± SEM combined from 2 (C), 3 (D,G), and

4 (F) independent experiments, or representative data from 2 independent experiments (E). $n = 5$ (C), $n = 3$ (D), $n = 5$-7 (F), and $n = 6$ (G). Results analyzed by one-way ANOVA and Dunnett's multiple comparisons test, which compared all time points to the 0 h non-treated (NT) control (C,D,F,G). *$p < 0.01$,***$p < 0.001$, ****$p < 0.0001$.

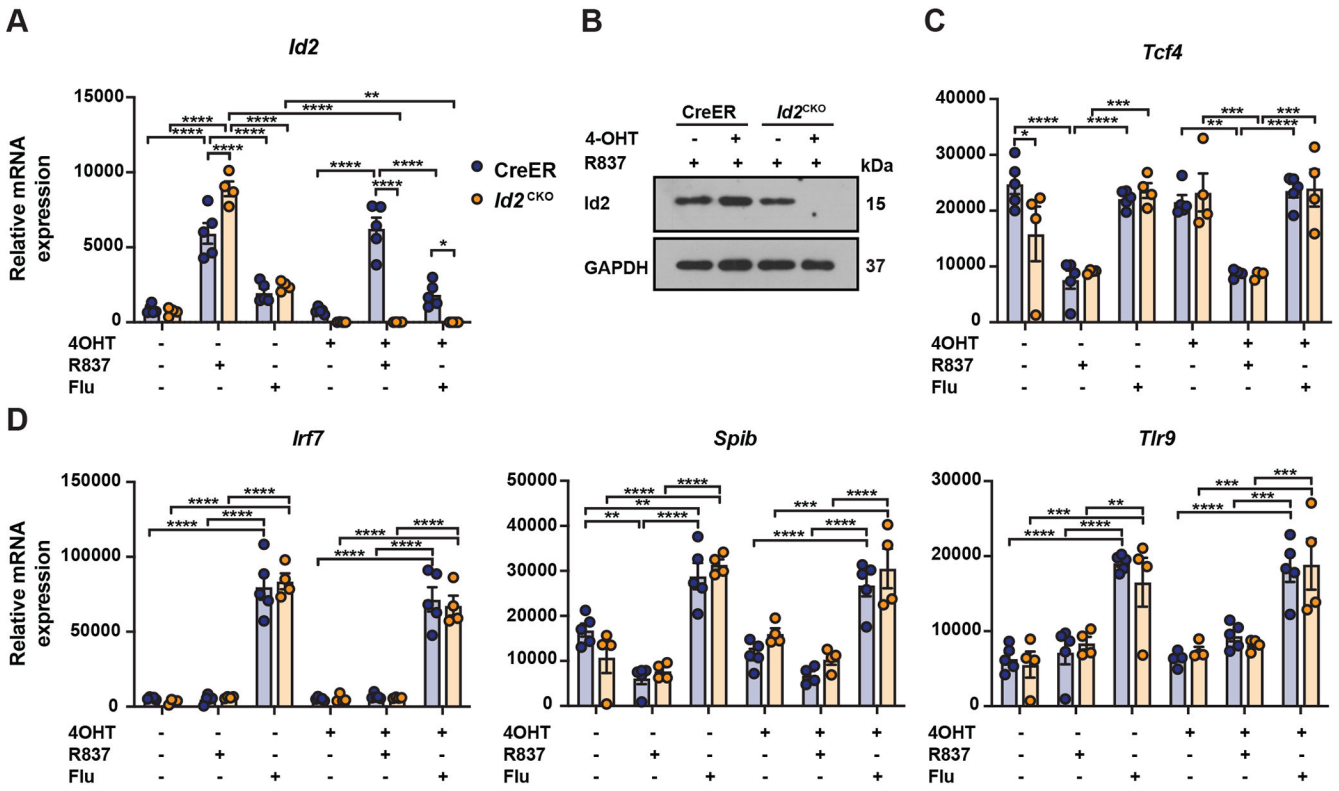

Figure 2: Loss of Id2 does not regulate *Tcf4* expression or E2-2 target gene expression following TLR7 activation *in vitro*.

(A-D) pDCs were differentiated *in vitro* from BM of CreER and CreER $Id2^{f/f}$ ($Id2^{CKO}$) mice. Cultures were treated on day 4 with 1 μM 4-OHT, and pDCs were subsequently treated with R837 (5 μg/mL) or heat-inactivated influenza virus (flu, MOI 50) in the presence of Flt3L (50 ng/mL) for 20-24, as indicated. (A) *Id2* mRNA expression, normalized to *Rpl13*. A value of "0" was used for $Id2^{CKO}$ samples whose expression of *Id2* was detected below threshold following 4-OHT treatment. (B) Representative immunoblot of whole cell lysates from pDCs treated with or without 4-OHT and R837 for 18 h. Id2 and GAPDH (loading control) were detected by antibody staining. (C) *Tcf4* mRNA expression, normalized to *Rpl13*. (D) *Irf7*, *Spib*, and *Tlr9* mRNA expression, normalized to *Rpl13*. Data shown as mean ± SEM combined from 2 independent experiments. $n = 4$-5 per genotype (A,C,D). Blots are representative of 2 independent repeats (B). Data analyzed by two-way ANOVA and Bonferroni's multiple comparisons test (A,C,D); significance shown for specified comparisons between genotypes of each treatment group, or comparisons within the same genotype between R837 or influenza treatment groups that did or did not receive 4-OHT. *$p < 0.05$, **$p < 0.01$, ***$p < 0.001$, ****$p < 0.0001$.

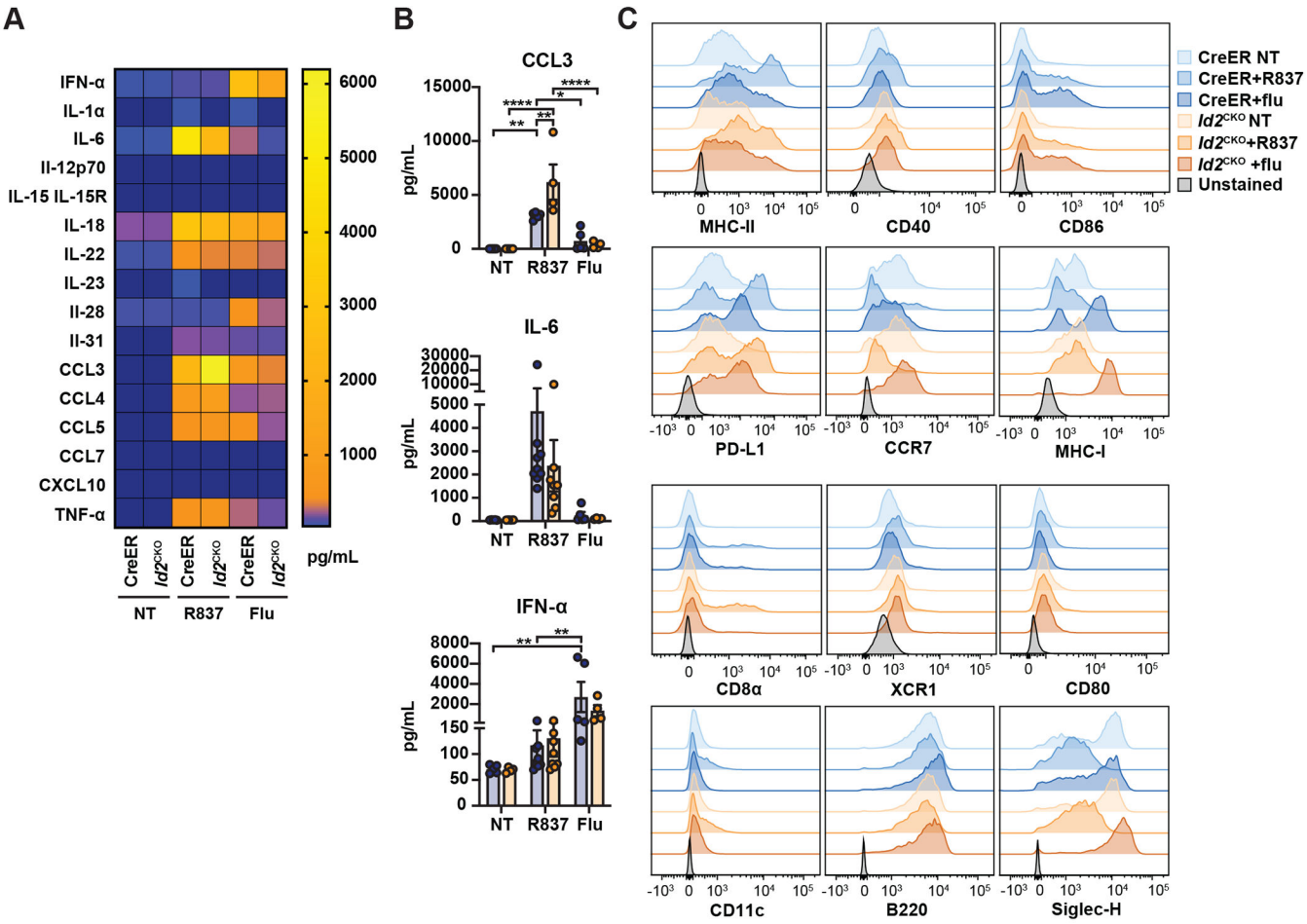

Figure 3. Id2-independent mechanisms contribute to TLR7-activated pDC soluble factor production and cell surface marker expression *in vitro*.

(A) Heat map of cytokine and chemokine amounts in cell cultures containing *Id2*^{CKO} pDCs or CreER pDCs. Cells in Flt3L (50 ng/mL) -containing cultures were treated with 4-OHT (1 μM) and supernatants were collected 18-24 h after addition of R837 (5 μg/mL) or heat-inactivated influenza virus (flu, MOI 50). Data show factors produced at least 2-fold higher in treatment groups compared to non-treated (NT) controls; factors produced outside of detectable limits of the multiplex assay or below 2-fold change from NT controls are not shown. (B) Amounts of CCL3, IL-6, and IFN-α (pg/mL) in pDC culture supernatants from the experiment summarized in A. (C) Representative histograms of cell surface marker expression on pDCs, following treatment with or without 4-OHT and R837 or influenza in the presence of Flt3L for 18-24 h, as indicated. Data shown as mean ± SEM combined from 2-4 (A,B) independent experiments, or representative of 2-5 (C) independent experiments. n = 3-9 (A,B) and n = 4-12 (C) per genotype. Data analyzed by two-way ANOVA and Bonferroni's multiple comparisons test; significance shown for comparisons between genotypes of each treatment group, and comparisons within the same genotype between treatment groups (B). *$p < 0.05$, **$p < 0.01$, ****$p < 0.0001$.

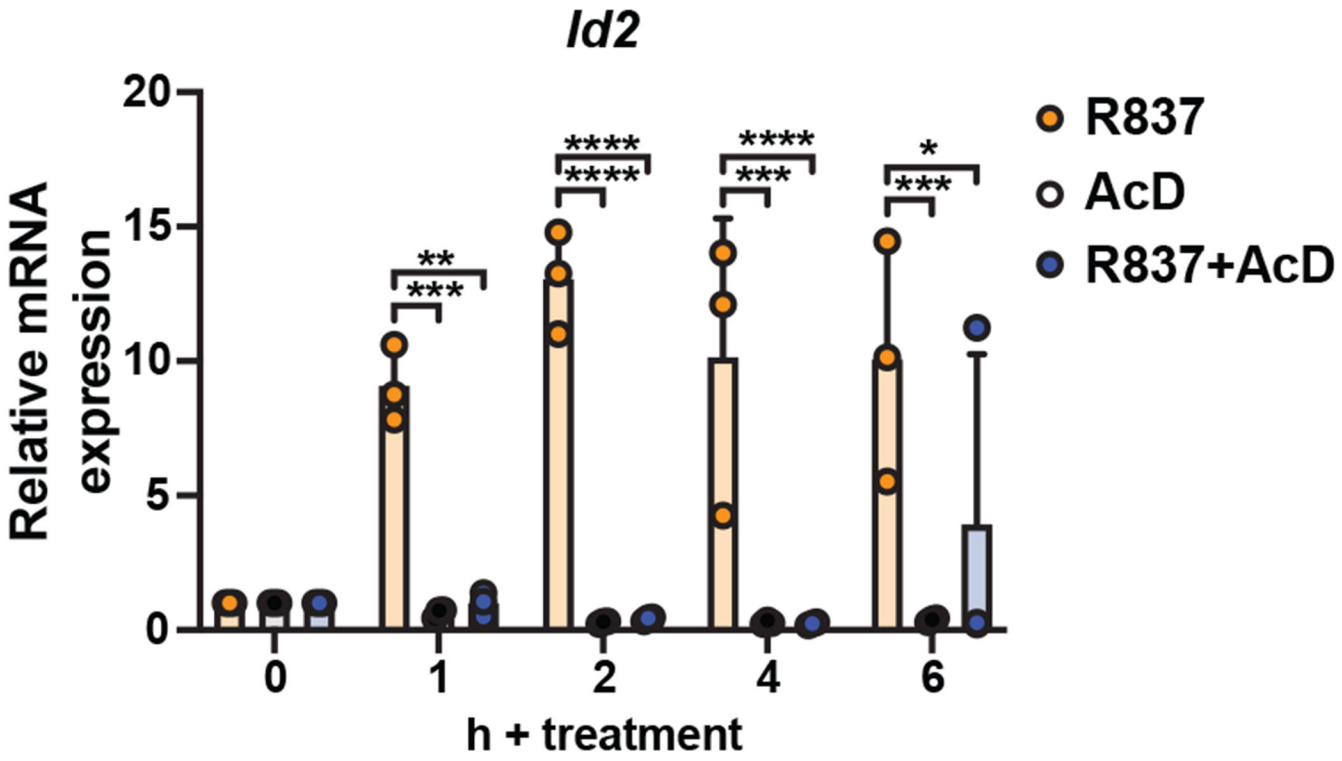

Figure 4. R837 stimulates *Id2* transcription.

pDCs were generated from BM of C57BL/6J mice by differentiation *in vitro*, and subsequently treated with R837 (5 μg/mL), Actinomycin-D (AcD, 5 μg/mL), or both for 1, 2, 4, and 6 h, as indicated. *Id2* mRNA expression was determined by RT-PCR; *Id2* expression normalized to *Rpl13*. Data shown represent mean ± SEM combined from 2 independent experiments. $n = 3$. Data were evaluated by two-way ANOVA and Tukey's multiple comparisons test; significance shows comparisons between treatment groups at each time point. *$p < 0.05$, **$p < 0.01$, ***$p < 0.001$, ****$p < 0.0001$.

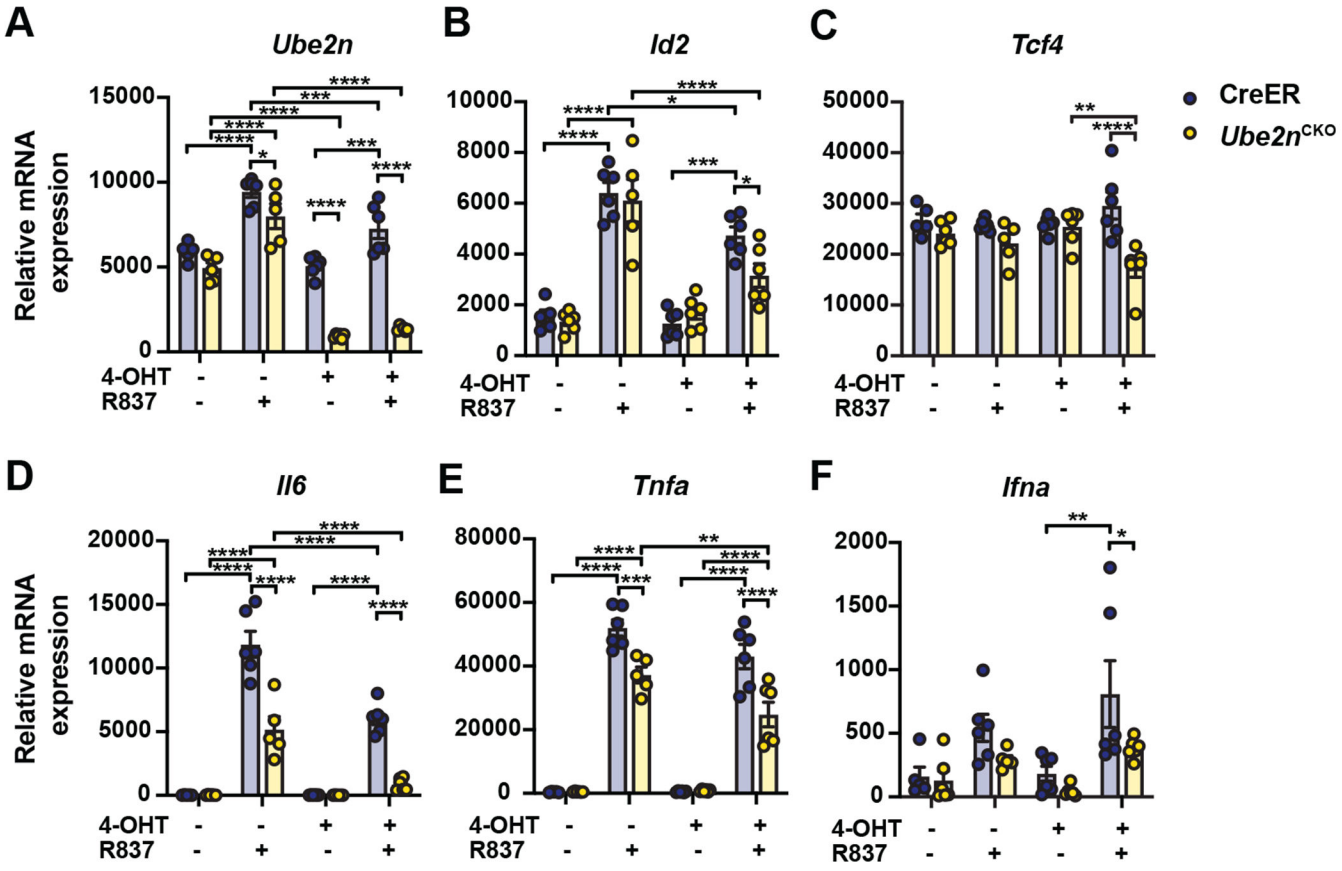

Figure 5. Ubc13 regulates *Id2* induction following R837 stimulation.

(A-F) pDCs were generated from BM of CreER or CreER *Ube2n*$^{fl/fl}$ (*Ube2n*^{CKO}) mice by differentiation *in vitro*. Cultures were treated on day 4 with 4-OHT (1 μM). Purified pDCs were stimulated with or without R837 (5 μg/mL) for 6 h, as indicated. *Ube2n* (A), *Id2* (B), *Tcf4* (C), *Il6* (D), *Tnfa* (E), and *Ifna* (F) mRNA expression was determined by RT-PCR; expression of each gene was normalized to *Rpl13*. Data shown represent mean ± SEM combined from 2 independent experiments. n = 5-6 per genotype. Data were evaluated by two-way ANOVA and Bonferroni's multiple comparisons test; significance shows comparisons between genotypes within treatment groups, or specified comparisons within the same genotype between R837 treatment groups that did not receive 4-OHT, or R837 treatment groups that received 4-OHT. *p < 0.05, **p < 0.01, ***p < 0.001, ****p < 0.0001.

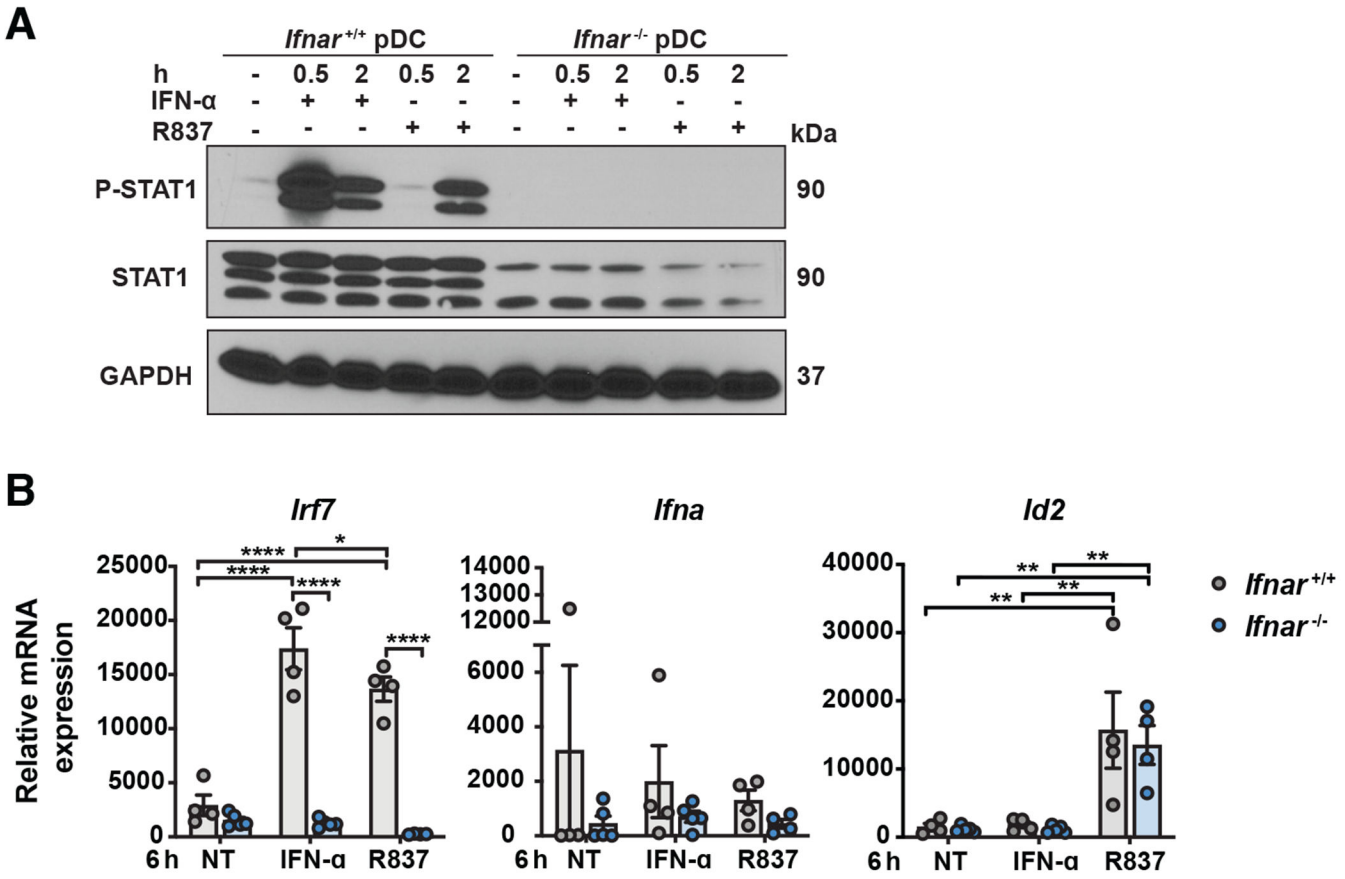

Figure 6. Induction of *Id2* by R837 is independent of IFNAR signaling.

(A) Representative immunoblot of phosphorylated-STAT1 (P-STAT1) and total STAT1 protein expression in C57BL/6J (*Ifnar*$^{+/+}$) and *Ifnar*$^{-/-}$ pDCs stimulated with or without IFN-α (300 units), R837 (5 μg/mL), or both for 0, 0.5, and 2 h, as indicated; GAPHD was used as loading control. (B) mRNA expression of *Irf7*, *Ifna*, and *Id2*, normalized to *Rpl13*, in pDCs stimulated with or without IFN-α or R837 for 6 h. Blot representative of 2 independent repeats (A). Data shown represent mean ± SEM combined from 3 (B) independent experiments. n = 4-5 per genotype (B). Data were evaluated by two-way ANOVA and Bonferroni's multiple comparisons test; significance shows comparisons between genotypes within treatment groups and differences between all treatments within each genotype (B). *$p < 0.05$, **$p < 0.01$, ****$p < 0.0001$.

Table 1.

qRT-PCR primer sequences.

Primer Name	Forward Primer (5’ to 3’)	Reverse Primer (5’ to 3’)
Ccl3	GTGGAATCTTCCGGCTGTAG	ACCATGACACTCTGCAACCA
Id2	CTCCTGGTGAAATGGCTGAT	GCTTATGTCGAATGATAGCAAAG
pan-*Ifna*	CCTGAGANAGAAGAAACACAGCC	GCTCTCCAGANTTCTGATCTG
Il6	CTGCAAGAGACTTCCATCCAG	AGTGGTATAGACAGGTCTGTTGG
Irf7	CCACGGAAAATAGGGAAGAAG	ACTAGAAAGCAGAGGGCTTGG
Rpl13a	GAGGTCGGGTGGAAGTACCA	TGCATCTTGGCCTTTTCCT
Spib	CCCCAGAGGACTTCACCAG	GGGCTGTCCAGCATAATGTC
Tcf4	AGACCAAGCTCCTGATTCTC	AGGCTCTGAGGACACCTTCT
Tlr9	ACAACTCTGACTTCGTCCACC	TCTGGGCTCAATGGTCATGT
Tnfa	AGGGTCTGGGCCATAGAACT	CCACCACGCTCTTCTGTCTAC
Ube2n	CAGAACCAGTTCCTGGCATT	CAGTGCTGGGGACCACTTAT